

smectite.

4) Coarse quartzdiorite (CQd)

a) Distribution

Coarse quartzdiorite (CQd) occurs as a dike intruded into a small intrusive body of melanocratic quartzdiorite.

b) Lithology

The rock (CQd) shows light gray to light brownish gray in color, massive and coarse grain. Color index of the rock (CQd) is 2 % to 3 % only. Chalcopyrite dissemination are recognized intensely in the rock body. As constituent minerals detected in naked eyes are plagioclase quartz and biotite. Biotite is substituted partly by some green alteration minerals such as chlorite, etc.

The microscopic characteristics of the rock (CQd) are as follows:

coarse quartzdiorite (CQd) (C3033)

Location: About 1 km south southeast of Ashuaca, along a branch river flowing to northwest

Texture: Holocrystalline, equigranular

Constituent minerals: Plagioclase biotite, quartz apatite, allanite, zircon, and opaque minerals

Alteration minerals: Muscovite (fine grained), albite, epidote, smectite

5) Porphyritic andesite (Pa)

a) Distribution

Porphyritic andesite crops out at 1,750 m in altitude along the ridge of Ashuaca, trending toward NE-SW direction.

b) Lithology

The rock (Pa) shows gray in color, porphyritic and compact. Plagioclase and hornblende are obvious as phenocrysts. Neither mineralization nor alteration are observed.

2-1-3 Geological structure

(1) Lineaments

Lineaments in the surveyed area were analyzed with aerial photograph of 1 to 60,000. The result are shown on a topographic map of 1 to 20,000 (Figure A-5).

The most prominent lineament detected on the aerial photograph is NW-SW one which

passes Telimbela village and directs toward northeast direction, next prominent one is E-W, a branch lineament of the former, which runs just south of Ashuaca. Other significant lineaments are mentioned as follows: NNW-SSE, NE-SW and ENE-WSW directions.

(2) Faults

Major lineaments analyzed are to be correspond to geological faults. For instance, one: NE-SW fault which passes telimbela village and directs toward northeast direction and two: E-W fault which is a branch of the former and runs along the river Q. Ugshacochoa, just south of Ashuaca. Two white argillized and silicified zones are both situated actually on the Fault lines which mentioned above.

Adding this surveyed area lies on or near a tectonic zone trending NE-SW direction where crossing the Frente de Banos fault which stretches from Guayaquil to Quito. Therefore, NW-SW lineament, a lineament of the same direction as the Frente de Banos fault, may be a product relating to the same tectonic movement.

2-1-4 Mineralization and alteration

Outcrops, which are mineralized of pyrite and chalcopyrite, are recognized along Q. Ugshacochoa, Q. Ashuaca and their branches. They are mainly and approximately distributed in an area of 1.5 km x 1.0 km near Ashuaca. This mineralized zone is called "Northeast mineralized zone" which is correspond to mineralized zones V and VI in the Phase II report. Intense mineralized area within the Northeast mineralized zone is concentrated in a limited area of 400 m x 600 m in the west of Ashuaca School, therefore called the "Ashuaca mineralized zone".

Northeast mineralized zone

(1) Type of mineralization

Type of mineralization recognized in the survey area is porphyry copper type.

(2) Occurrence

In the area mineralized are all type of rocks including not only granitic ones but also the Macuchi Formation. Furthermore, molybdenite is recognized where intense chalcopyrite and pyrite mineralization and where high ratio of chalcopyrite/pyrite. Fig.II-2-4 shows a sketch of a mineralized outcrop along Q. Ugshacochoa in Ashuaca mineralized zone. Five more mineralized outcrops are observed, which are also good mineral showings.

Sulfides occur differently between inner and outer part of the mineralized zone. The

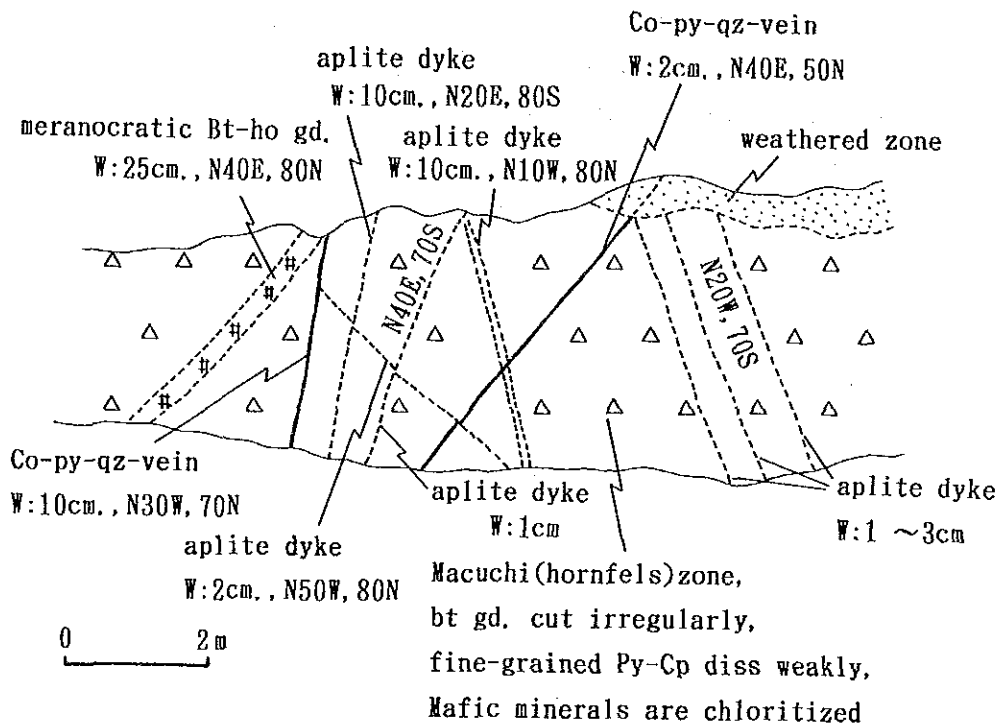


Fig.II-2-4 Geologic sketch of a mineralized outcrop in ZONE V

former, the mineralization are of chalcopyrite and pyrite in forms of spotted, film and/or veinlets, and the mineral assemblages of chalco-pyrite-pyrite-quartz veins are common. In the latter, contrary, they are in a form of dissemination along cracks only. Content of ore minerals decreases here.

Assay result of ore samples from the Northeast mineralized zone were 0.71 to 1.38 % Cu in the central part and less than 0.1 % in the outer part, where pyrite dominates in forms of dissemination and/or veinlets. Pyrite is more abundant in southern part than in other parts.

Pit survey is also adopted in an area of Ashuaca, because surface is covered by thick weathered soil. Dissemination and veinlets of limonite are observed commonly in every pit, one of which contained a grain of malachite. Cu content of samples collected from pits was distinctively higher than that of background. The highest one was 0.51 % Cu. Therefore Cu content in the samples from pits indicates that pit exists in an area mineralized intensely of chalcopyrite and that the samples properly acquired chalcopyrite and/or its oxidized minerals which were contained in the country rocks.

Alteration associated with mineralization are strong silicification and chloritization.

(3) Structure control

Northeast mineralized zone distributes in the vicinity of NE-SW fault along Q. Telimbela-Q. Ashuaca and of E-W fault along Q. Ugshacocha. Furthermore "Ashuaca mineralized zone", a intense mineralized zone, occupies in the vicinity of intersection of those two faults mentioned above.

Most of lineaments, which develop in the survey area, are considered to be related to the activities of the tectonic line, the Frente de Banos fault, because it traverses nearby the survey area and trends toward NE-SW direction.

This assumption is supported by the facts that numbers of stocks and dikes are concentrated in the surveyed area, and their number is more than that of any other project areas in bolivar region, and that their distribution is also and/or elongation of intrusion controlled in the NE-SW direction.

2-1-5 Magnetic susceptibility measurement

To determine the demagnetization due to mineralization quantitatively, magnetic susceptibility was measured with a portable magnetometer through the geological survey route. The magnetometer used was "Kappameter Model KT-5" made in Czechoslovakia, measurement sensitivity was 1×10^{-3} SIU.

At the measurement, some efforts were made to avoid measuring errors due to weathering and irregular surface that were to scrape weathered portions off completely and to make surface smooth and flat. Measurement of magnetic susceptibility was repeated five times generally at one measurement station and adopted mean of three values inside by omitting outer ones, maximum and minimum.

Distribution of measurement station and measured magnetic susceptibilities are shown in Figure A-2.

Each magnetic susceptibility of rocks in the surveyed area showed the intensity of rock itself un-demagnetized as recognized in the Osohuayco zone of Balzapamba area. It seemed to be difficult to delineate demagnetized zone associated with mineralization through processing data detected quantitatively.

2-2 Geophysical survey

2-2-1 Purpose of survey

The purpose of this survey is to clarify the lateral and vertical extension of the mineralization detected by the Phase II Survey in the northeastern zone of Telimbela area. To meet the above, an investigation of the electrical structure of the area was carried out by clarifying the distribution of IP anomalies in the survey area by means of a conventional IP method.

2-2-2 Survey method

(1) IP method

An IP (Induced Polarization) method is a geophysical technique that measures the polarization effects caused by the electrochemical nature of the minerals and rocks. This method has been mainly utilized for detecting sulphide deposits.

There exist four measuring methods to observe an IP phenomenon, i.e.,

1) Frequency-domain

When using the frequency-domain method, the magnitude of the IP phenomenon is expressed by the parameter called Frequency Effect (FE) which is proportional to the resistivity difference at two frequencies.

2) Time-domain

In this method, the magnitude of the IP effect is expressed by the Chargeability which is determined by observing the transient voltage curve after the electric current is turned off.

3) Phase-domain

The magnitude of the IP phenomenon in the phase-domain method is expressed in terms of the difference of the phase angle between the transmitted and received signals.

4) Spectral IP

The magnitude of the IP phenomenon is here expressed as the normalized amplitude and phase in each frequency referred to the lowest frequency among a wide variation of frequencies.

(2) Measurement method

The measurements were done by using the frequency-domain method at the frequencies of 3.0Hz and 0.3Hz and adopting a dipole-dipole electrode configuration with a separation factor n from 1 to 5.

Based upon the geological structure, six survey lines of 1600m each in length were set along a NW-SE direction with a 300m line spacing. The numbering of the points were set one by one from 0 to 32 with a 50m interval from the northwest end of each line and the measurements were done every 100m spacing with a 100m potential electrode.

The location of survey lines are illustrated in Fig.II-2-5.

(3) Survey instruments

Instruments used for the conventional IP survey were manufactured in Japan, with the exception of an engine generator which was manufactured in Canada, are shown below

Equipment	Model	Specification	Quantity
IP Transmitter	CH-T7802	2.5A, 800V	1
IP Receiver	CH-R7802		1
IP Checker	522A		1
Engine Generator	GPU-2000	2kw,150V,400Hz	1
Electrode Remote Controller	CH-60A	64ch	1
Transceiver	ICB-660	0.5W	6

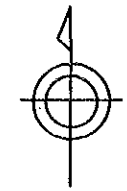
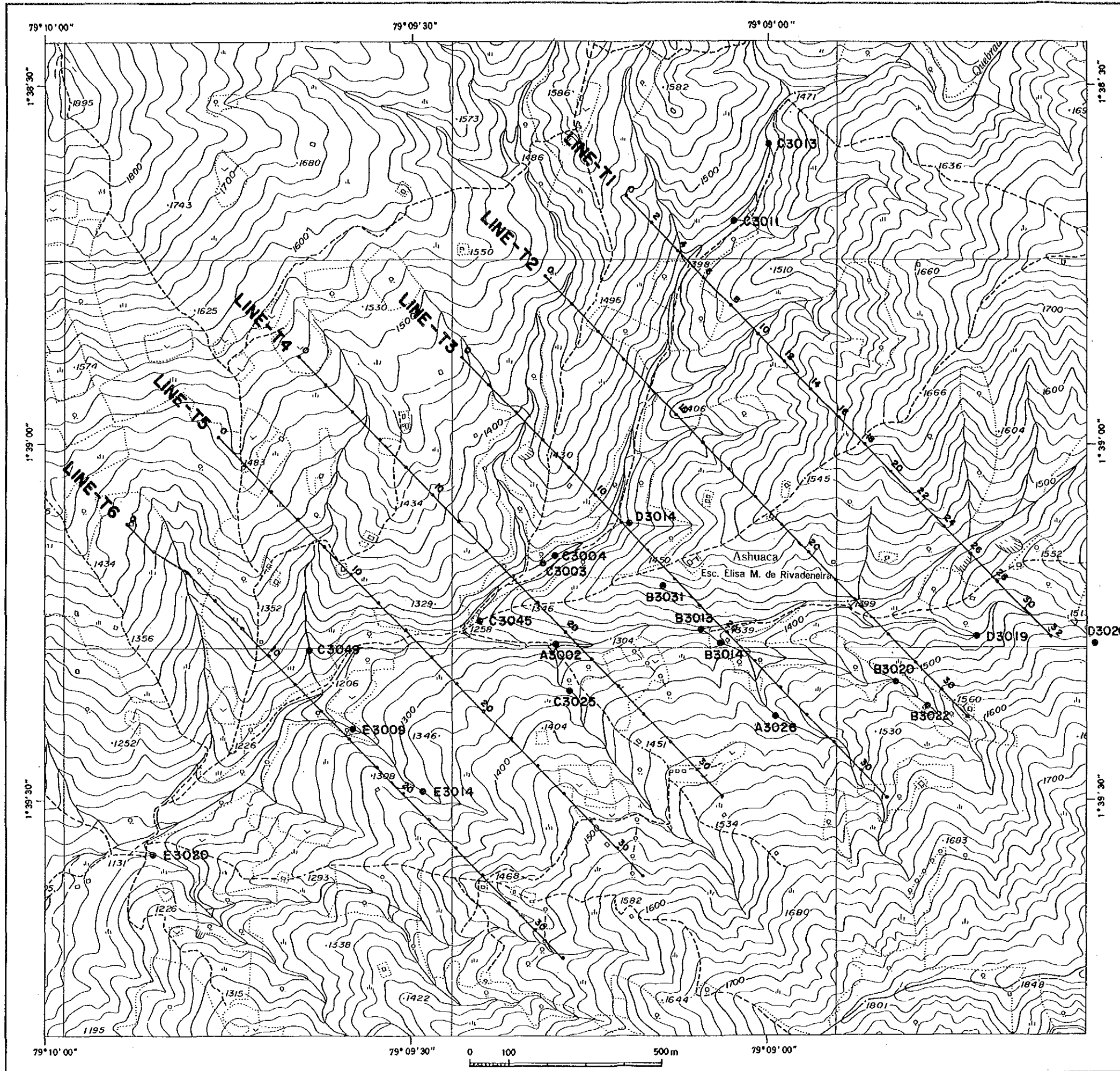
2-2-3 Analysis method

Fig.II-2-6 shows a procedure for data analysis.

(1) Calculation of apparent resistivity and frequency

The measurement is conducted by supplying electric current (I_{ac}) at 3.0Hz into the ground through a pair of current electrodes (C_1, C_2) and detecting the corresponding potential difference (V_{ac}) with a pair of potential electrodes (P_1, P_2).

The apparent resistivity (APR) of the ground is calculated by applying the measured potential difference to the following equation:



LEGEND

- LINE-T3 IP Survey Line
- C3045 Location of Rock Sample and Sample Number

Fig.II-2-5 Location map of IP survey lines of the Telimbela area

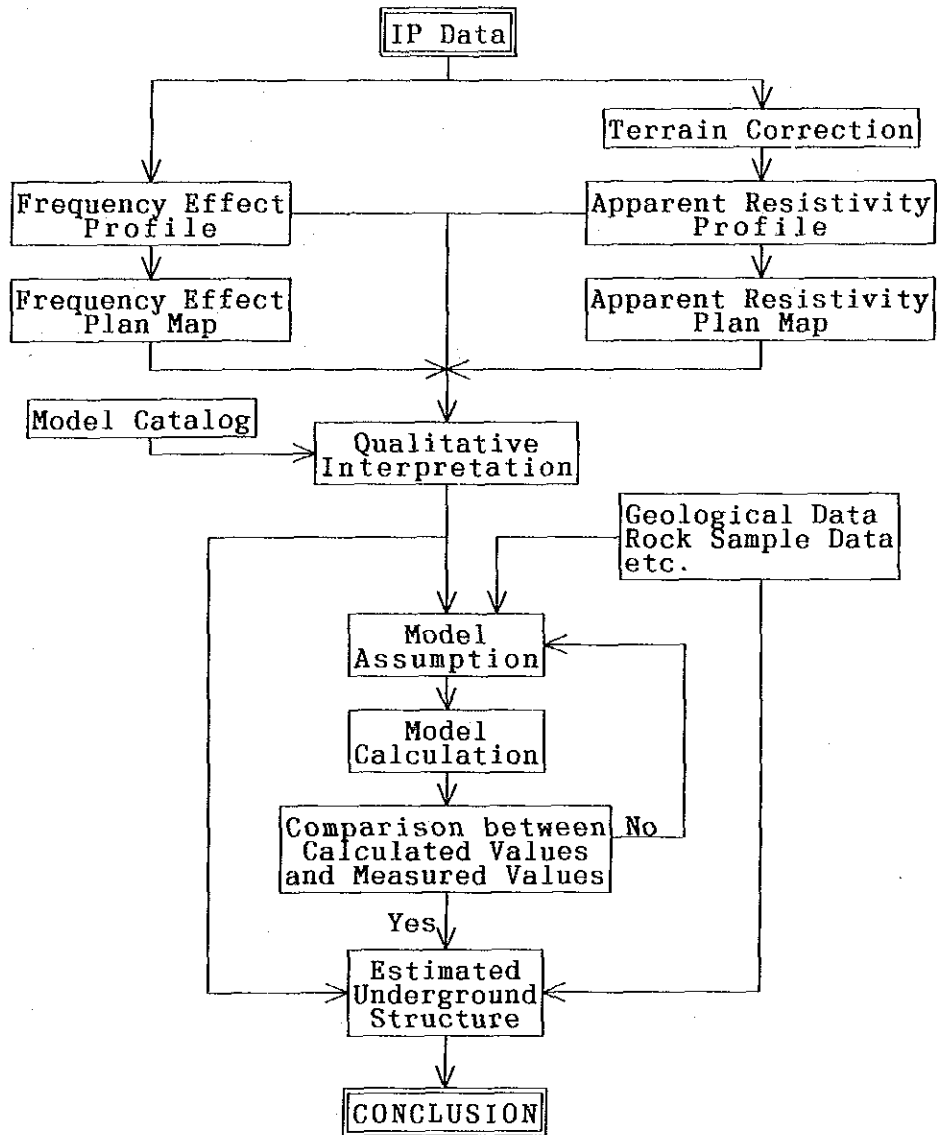


Fig.II-2-6 Flow chart of IP data analysis

$$APR = K \cdot \frac{V_{ac}}{I_{ac}} \quad (\Omega \cdot m)$$

K is a geometric factor which depends on the electrodic configuration utilized.

$$K = 2\pi / \left(\frac{1}{C1P1} - \frac{1}{C1P2} - \frac{1}{C2P1} + \frac{1}{C2P2} \right)$$

After reading the potential difference Vac at 3.0 Hz, the frequency is changed to 0.3Hz while the current is kept constant. The frequency effect (FE) can then be directly read by a meter of a receiver panel and calculated by the following formula, which is also a function of the change in resistivity as the frequency is changed.

$$FE = \frac{V_{dc} - V_{ac}}{V_{ac}} \times 100 = \frac{\rho_{dc} - \rho_{ac}}{\rho_{ac}} \times 100 \quad (\%)$$

The value of APR and FE are plotted at the intersection of lines extending downward at 45° angles from the transmitter and receiver midpoints. Since the depth of plotting does not represent the physical property with depth, this pseudo-section does not give a true section of the subsurface distribution of the IP effect.

(2) Terrain correction

Since the geometrical factor K is calculated as a function of the location of the current and potential electrodes on a half-infinite plane, APR is affected by topography depending on the location of electrodes, even if the terrain is homogeneous. For example, for the case of a dipole-dipole configuration, APR appears to be high beneath a hill and low beneath a valley. On the other hand, FE is less affected by topography because it is rather proportional to the ratio of resistivity differences at two frequencies.

As the topography of the survey area is comparatively steep and rugged, the correction was performed for all survey lines by means of a finite element method assuming a two dimensional half space topography.

The pseudo-sections and plan maps were drawn using the topography corrected values.

(3) Electrical measurement of rock samples

Electrical measurements on rock samples were carried out in order to determine the actual electrical properties of rocks distributed on the survey area.

The rocks collected from the surface were formed into a cubic shape while the rocks collected from the drill holes were cut into 3 to 5 cm length. Their measurements were realized in water saturated condition after the rocks were soaked in water during ten days.

The resistivities of the rock sample are calculated by the following equation:

$$\rho = \frac{a_1 \times a_2}{\ell} \times \frac{V}{I}$$

ℓ : thickness of sample (m)
 a_1, a_2 : width of sample (m)
 V : potential difference (V)
 I : electric current (A)

As same as for the case of field survey, FE was calculated by using the resistivity differences at 0.3Hz and 3.0Hz.

(4) Simulation analysis

For analysis of IP data, there are mainly two methods:

One is a qualitative method which correlates the anomaly patterns of profile and plan map in reference to standard anomaly patterns derived from various simple physical structural models.

The other one is a quantitative method which compares the observed data with theoretical data calculated from the simulated physical structure.

The two methods were combined to obtain better results. Pseudosections were modeled by using meshes which assumes FE and resistivity values on the basis of geology, standard models and results of electrical measurement of rock samples. The theoretical values were then calculated by numerical analysis using a two-dimensional finite element computer technique.

Thereafter, comparisons between the calculated values and observed data permitted to change the various parameters of the model in order to approach efficiently the observed values. By this iterative procedure, it was possible to obtain an optimum model of the underground physical structure.

Simulation analysis was carried out for Line T-3, to clarify the lateral extension (NW-SE direction) of the Ashuaca mineralized zone.

2-2-4 Results of survey and interpretation

(1) Results of rock sample measurement

Resistivity and FE values were measured for 21 rock samples collected in the northeastern part of Telimbela Area.

Locations of collected samples are shown in Fig.II-2-5, and the results of sample measurement are shown in Table II-2-1.

Table II-2-1 Resistivity and FE of rock samples in the Telimbela area

No.	Sample No.	Rock Name	Occurance	ρ (Ω·m)	FE(%)
1	A 3002	hornfels	partly (cp)-py-qtz thin vein	735	5.4
2	A 3026	andesite	py-cp in crack, sili.	2,134	3.4
3	C 3025	andestic tuff	py-cp-qtz thin vein, sili.	2,299	7.8
4	C 3049	basaltic andesite	py in crack, sili	2,330	3.8
5	E 3009	andesite	py-cp in crack & diss., chl.	856	7.1
6	E 3020	andestic tuff	py in crack, sili.	4,900	4.3
7	B 3014	ho qtz-diorite	weakly py diss.& film	4,339	2.1
8	B 3031	ho qtz-diorite	v.wk py diss., chl. arg.	795	8.4
9	C 3003	ho qtz-diorite	py-cp diss.& film	1,267	4.9
10	C 3004	ho qtz-diorite	str.py-cp-mo diss.& film, chl.	251	38.0
11	D 3019	ho qtz-diorite	py diss, chl.	615	8.2
12	A 3030	quartz-diorite	weakly mineralization	3,520	2.2
13	B 3020	quartz-diorite	str.py-cp-mo diss.& film, chl.	711	14.8
14	B 3022	quartz-diorite	str.py-cp-mo diss.& film, chl.	517	23.0
15	C 3011	quartz-diorite	non mineralization	9,168	2.1
16	D 3020	quartz-diorite	py-cp diss.	3,500	4.6
17	B 3013	melanocratic qtz-dio.	py diss.& film	961	4.1
18	C 3045	melanocratic qtz-dio.	weakly py diss., sili.	3,051	2.8
19	D 3014	melanocratic qtz-dio.	strongly py-cp diss.	1,042	7.8
20	E 3014	melanocratic qtz-dio.	py-cp in qtz veinlet, chl.	1,868	3.8
21	C 3013	silicificated rock	strongly py diss.& film	682	22.5

dio. : diorite py : pyrite diss. : dissemination arg. : argillization
 qtz : quartz cp : chalcopyrite sili. : silicification str. : strongly
 ho : hornblende mo : molybdenum chl. : chloritization v.wk : very weakly

The resistivity of intrusive rocks (No.7-20) range from 251 to 9,168 ohm-m and Macuchi formation (No.1-6) from 735 to 4,900 ohm-m. Accordingly, it is difficult to identify the rock faces from the resistivity point of view as intrusive rocks change within a big range.

However, the scale of alteration of the geologic structures can be somewhat identified by their resistivity changes. In other words, resistivity values of the argillized rocks (mainly chloritization) are less than 1,000 ohm-m, and those of silicified rocks (which belong to Macuchi formation) are more than 2,000 ohm-m.

The FE values which are generally indicative of sulfide content can not be useful as a parameter for discriminating rock faces. Except for the strongly mineralized samples Nos.10, 13, 14 and 21, intrusive rock samples show 2.1 to 8.4% of FE, and Macuchi formation, 3.4 to 7.8% of FE. The minimum FE value of Macuchi formation which is higher than that of intrusive rock is due mainly to the mineralized rocks. However, the FE values of Macuchi formation will be lower than intrusive rocks, that depend on the results of the Phase II survey (Osohuayco zone of Balsapamba area). The highly mineralized rocks present a tendency of showing higher FE values being the highest values encountered in the chloritized rocks.

It is therefore concluded that the rock samples indicating low resistivity and high FE values represent the mineralized zone of this area. The resistivity values range from low resistivity and high FE for chloritized and strong mineralization rocks, to high resistivity and low FE for silicified and low mineralized rocks.

It can be also noted that rock samples Nos.10, 13 and 14 with molybdenum dissemination show abnormally high FE values, indicating much more sulfide mineralization content.

(2) Distribution of apparent resistivity (Fig.II-2-7, Fig.II-2-8, Fig.II-2-9, A-6)

Apparent resistivity for this district ranges from 38 to 3,370 ohm-m with a logarithmic average of 349 ohm-m. Here, for convenience' sake, resistivity of more than 1,000 ohm-m is called as high resistivity, 150 to 1,000 ohm-m as medium resistivity and less than 150 ohm-m as low resistivity.

As there appear to be a tendency of encountering high apparent resistivity in the north and low in the south, a boundary can be drawn from station No.10 on Line T-6 to No.24 on Line T-2 in E-W direction which coincide well with an assumed fault along the creek in the south of Ashuaca that runs in the same direction.

Another small scale resistivity boundary is assumed in the area from No.8 on Line T-1 to No.5 on Line T-5.

Smaller scale resistivity anomalies as seen in the Chaso Juan area and the Osohuayco zone of Balsapamba area (in the Phase II), are dominant in this zone, suggesting not only that geology here consist mainly of small intrusive rocks and small scale of geology, but also that different kind of alteration zones are in this zone.

High resistivity anomaly (H1) is seen in the northwestern end of Lines T-1 and T-2. Judging from Apparent Resistivity Pseudo-Section (Fig.II-2-9), a resistive body from shallow to the depth is suggested to correspond to silicified or not altered quartz diorite in that area.

In the southeast of this anomaly (Macuchi formation zone), from No.10 on Line T-1 to No.14 on Line T-4, a high resistivity (H2) is seen at the depths deeper than $n=3$, suggesting a buried resistive body formed by silicification along the fault.

On the other hand, low resistivity anomalies are seen elsewhere reflecting a shallow or surface conductive layer due to argillization (chloritization and montorillonitization).

Low resistivity anomalies of less than 250 ohm-m seen in the south from No.20 on Line T-1 to No.26 on Line T-3 correspond to the distribution of melanocratic quartz diorite located the south of Q.Ugshacocha. Among them, L3 and L6 are due to the surface or shallow sources as indicated by typical pants-leg shaped anomalies, reflecting the strongly chloritized part of melanocratic quartz diorite.

The three low resistivity anomalies I4, L5 and L7, seen in Macuchi Formation area, are all considered to be reflecting shallow or surface chloritization.

Furthermore, low resistivity anomalies seen from No.12 on Line T-3 to No.15 on Line T-4 (the northwest of Ashuaca), and from No.25 on Line T-2 to No.22 on Line T-4 (the southeast of Ashuaca) in plan map of $n=1$ correspond to the parts strongly disseminated with pyrite-chalcopyrite of Ashuaca mineralized zone.

(3) Distribution of FE (Fig.II-2-10, Fig.II-2-11, Fig.II-2-12 A-7)

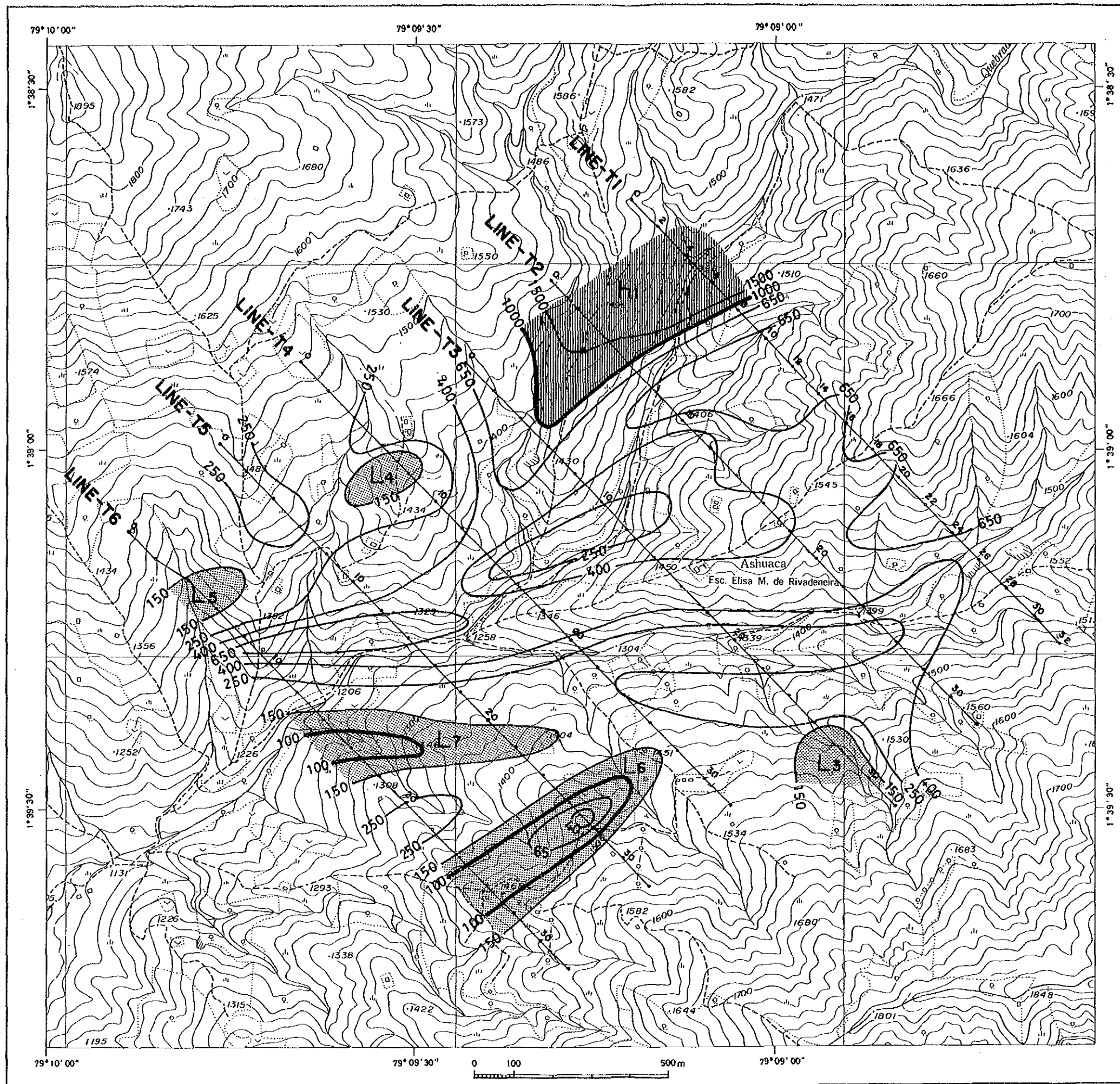
In this section, distribution of FE of more than 8% is called high FE, from 5 to 8% medium FE and less than 5% low FE.

In general, low FE is dominant in the central district towards northwest, surrounded by high FE anomalies.

Low FE detected in northwestern district extending to the depths (on Lines T-3, T-4 and T-5) seems to reflect Macuchi formation without mineralization.

Intrusive rocks in this zone is generally pyrite disseminated showing more than 5% FE. Among them, melanocratic quartz diorite shows the highest FE indicated by the high FE anomalies II and IV, which are due to strongly pyrite dissemination and chloritization.

The area where Macuchi formation is distributed, a high FE anomaly III was detected on Line T-6 with No.12 as its center and which correspond to an area characterized by highly mineralization and chloritization. This anomaly is caused by a typical shallow source, suggesting a shallow and thin layer near the surface.



LEGEND



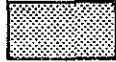
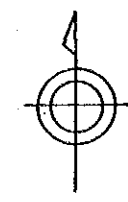
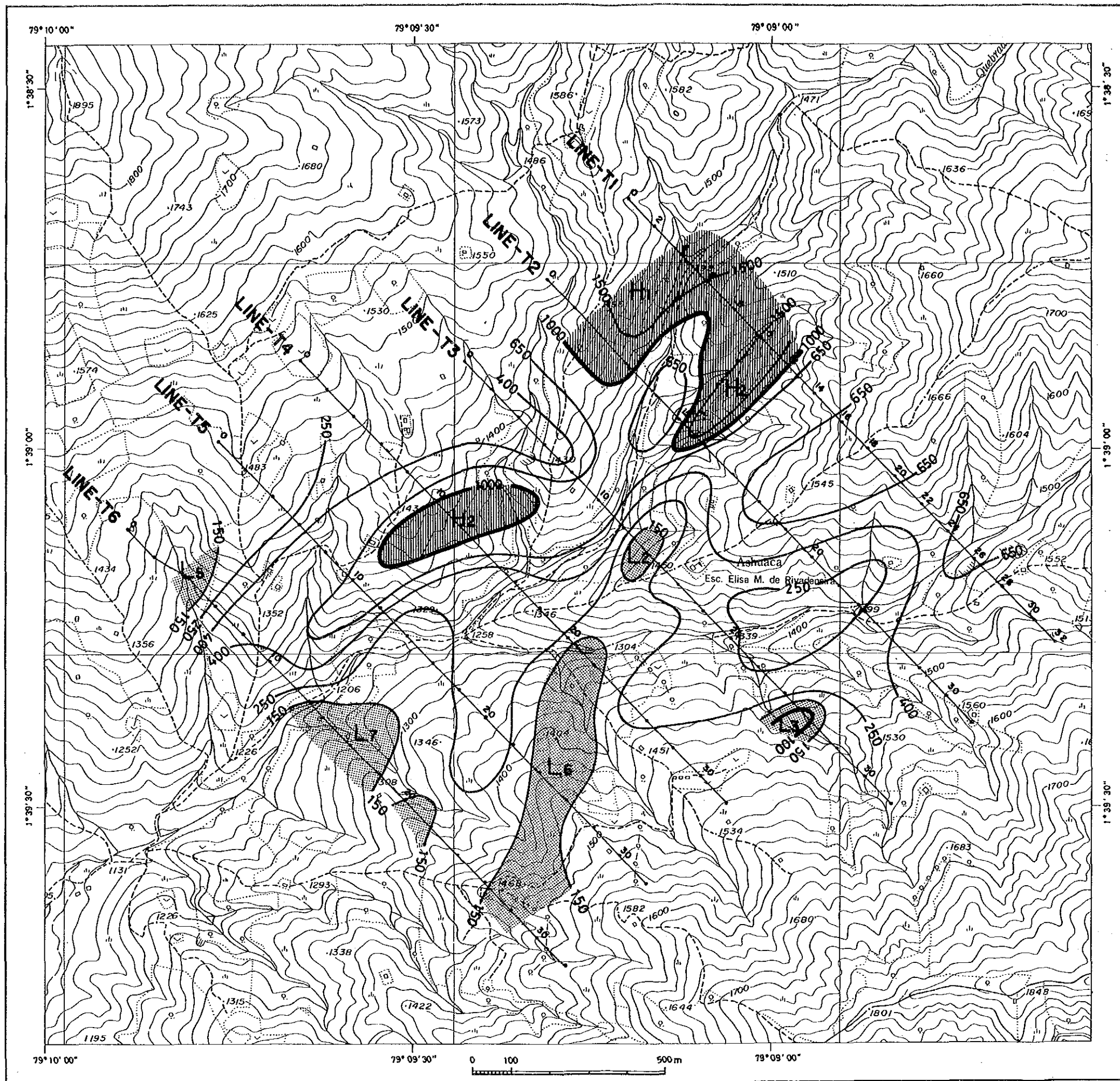
-  $1,000 \leq \rho_a$
 -  $150 \leq \rho_a < 1,000$
 -  $\rho_a < 150$
- UNIT: $\Omega \cdot m$

Fig.II-2-7 Apparent resistivity plan map($n=1$) of the Telimbela area



LEGEND


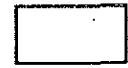
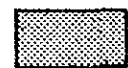
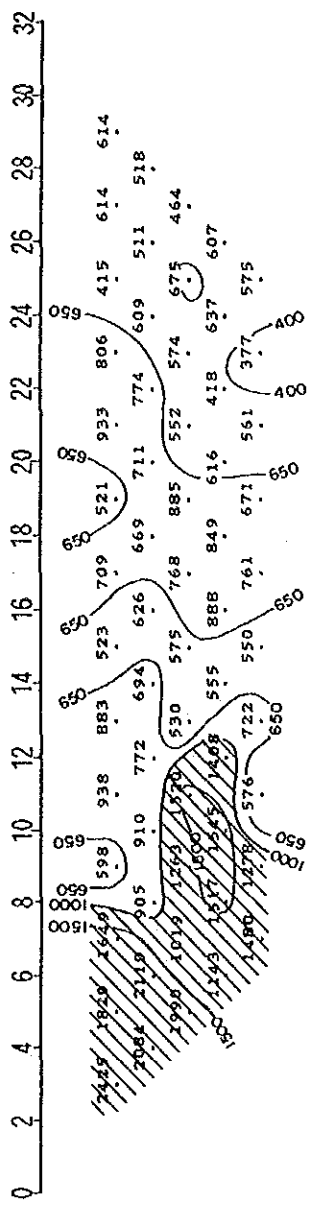
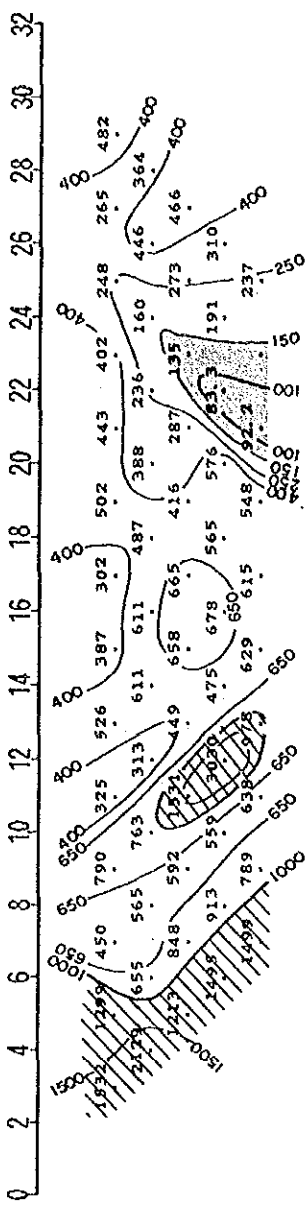
-  $1,000 \leq \rho_a$
 -  $150 \leq \rho_a < 1,000$
 -  $\rho_a < 150$
- UNIT: $\Omega \cdot m$

Fig.II-2-8 Apparent resistivity plan map(N=3) of the Telimbela area

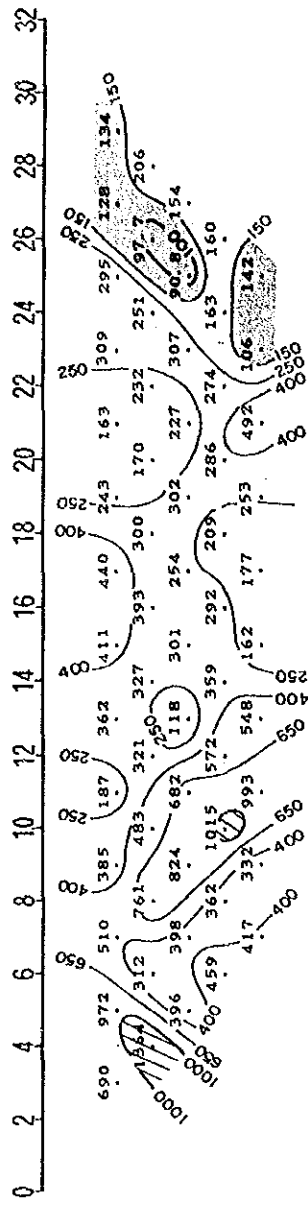
LINE T-1



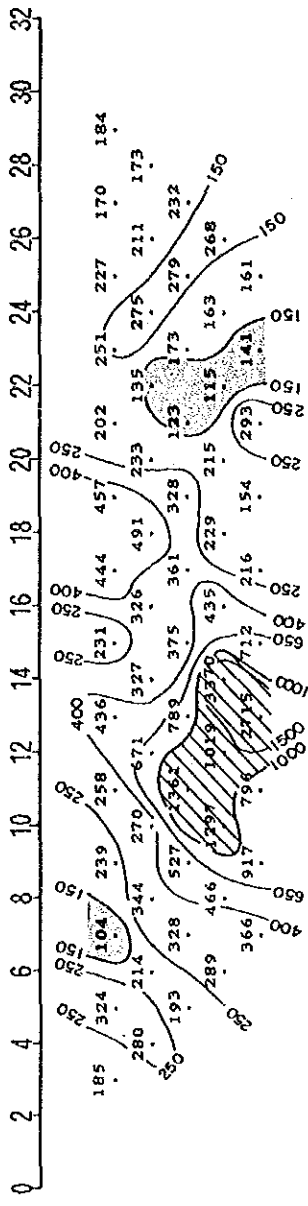
LINE T-2



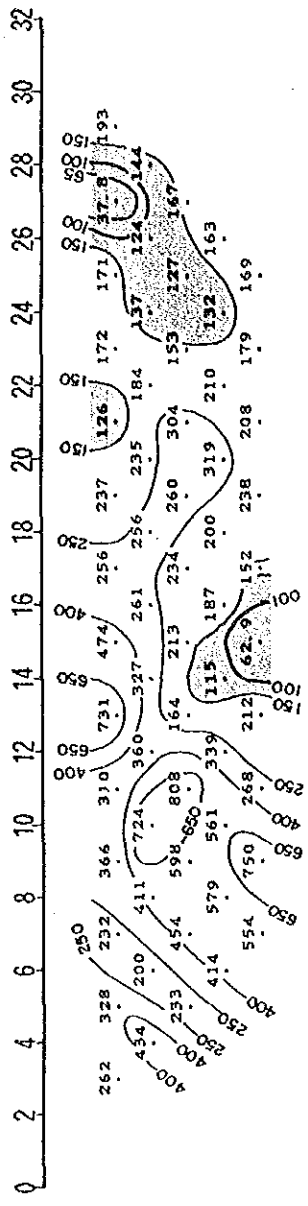
LINE T-3



LINE T-4



LINE T-5



LINE T-6

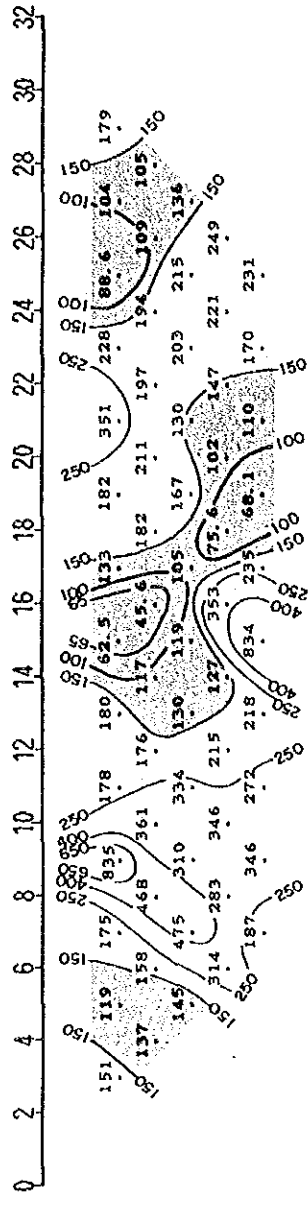
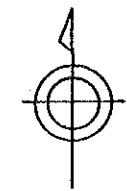
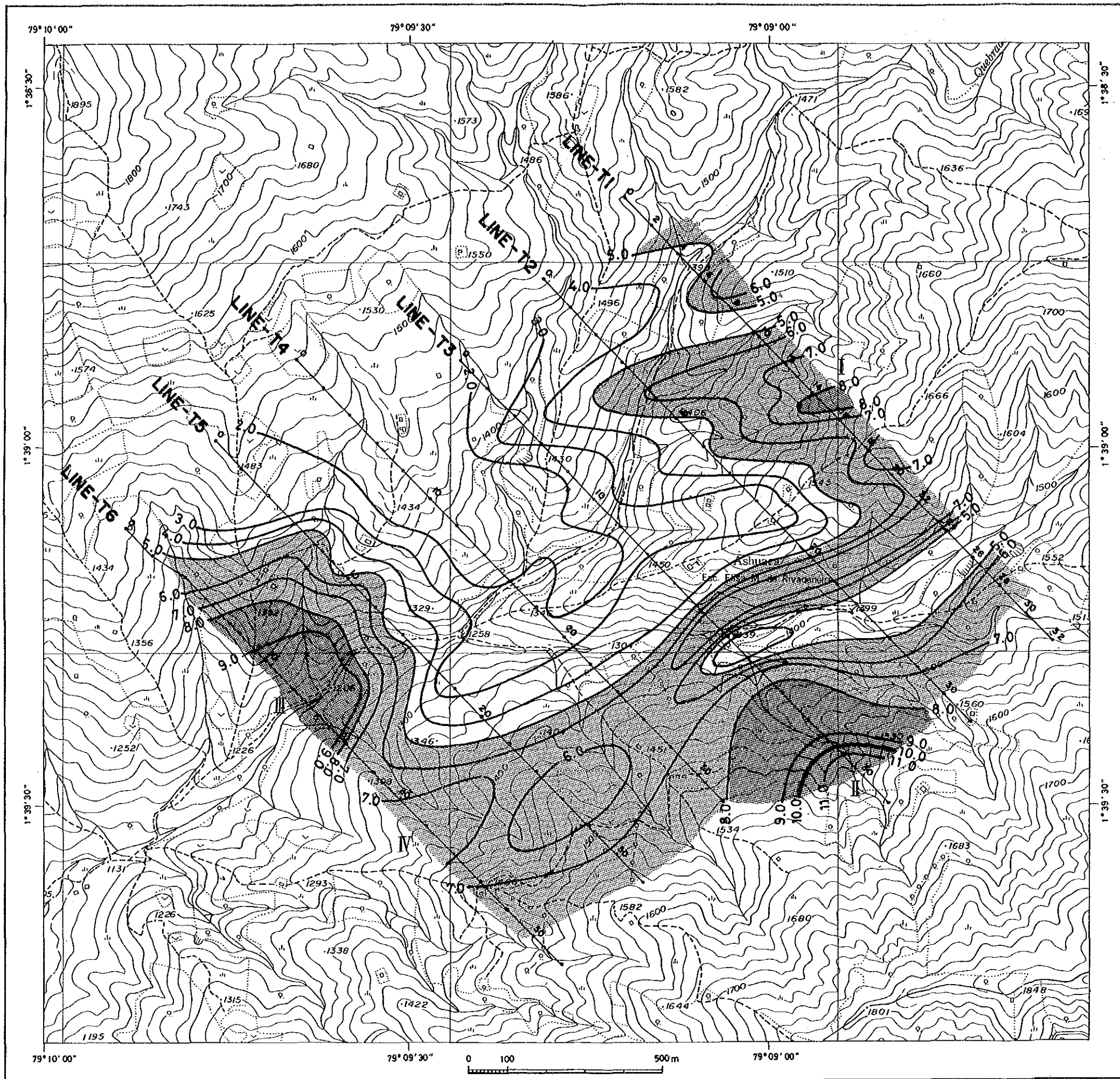


Fig. II-2-9 Pseudo-sections of apparent resistivity



LEGEND


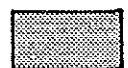

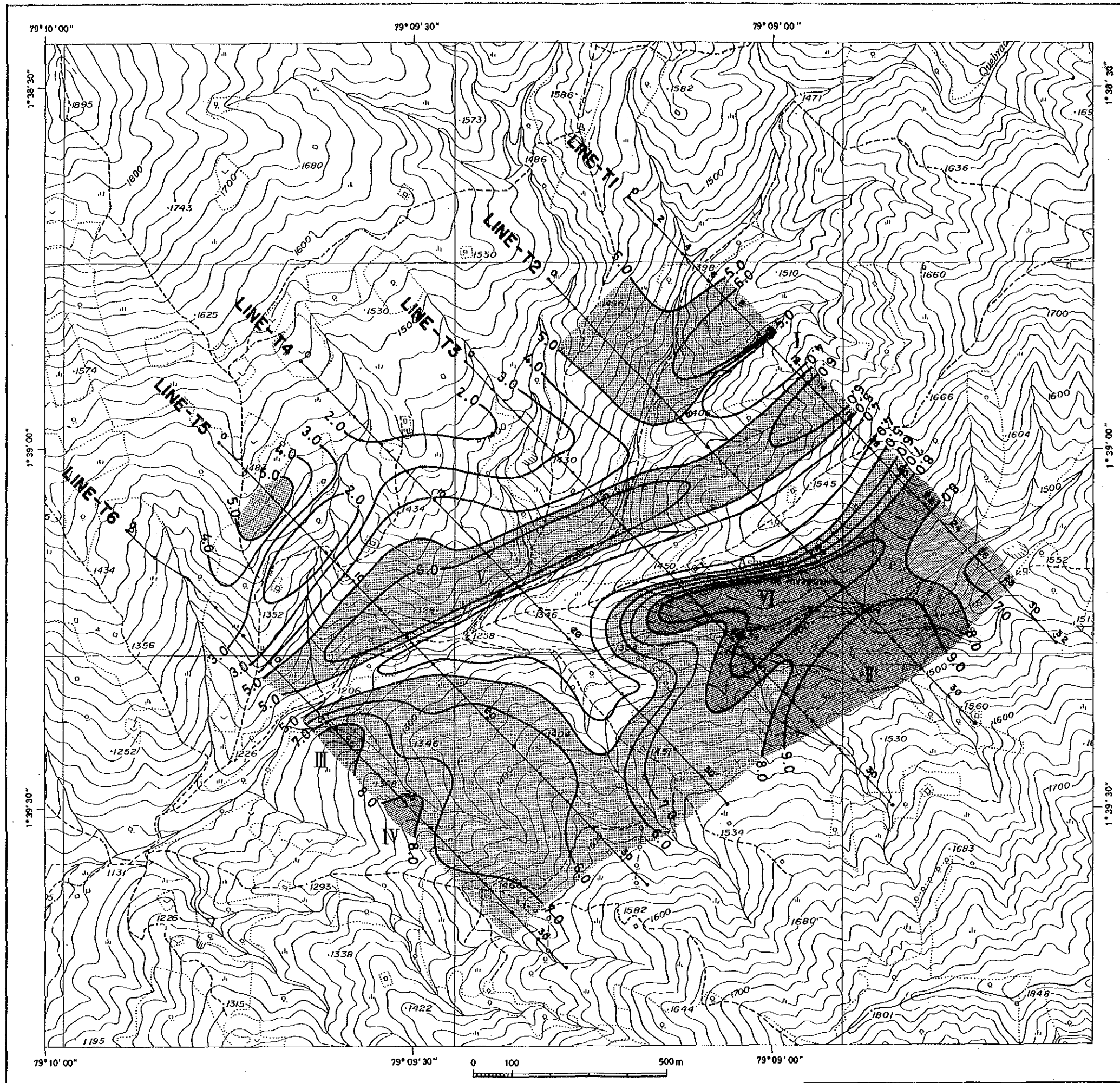
-  8.0 ≤ PFE
 -  5.0 ≤ PFE < 8.0
 -  PFE < 5.0
- UNIT : %

Fig.II-2-10 FE plan map(n=1) of the Telimbela area



LEGEND

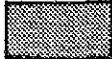

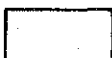
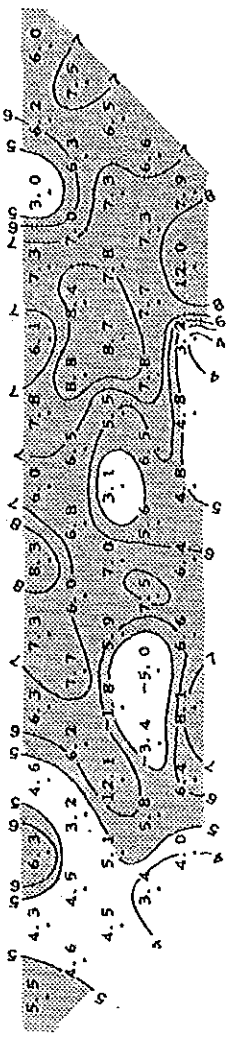
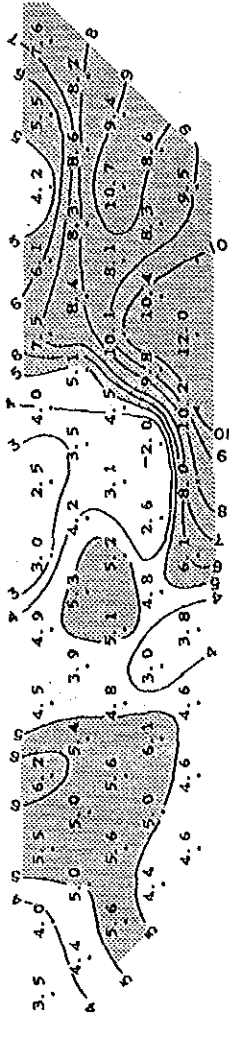
-  $8.0 \leq \text{PFE}$
 -  $5.0 \leq \text{PFE} < 8.0$
 -  $\text{PFE} < 5.0$
- UNIT : %

Fig.II-2-11 FE plan map(n=3)
of the Telimbela area

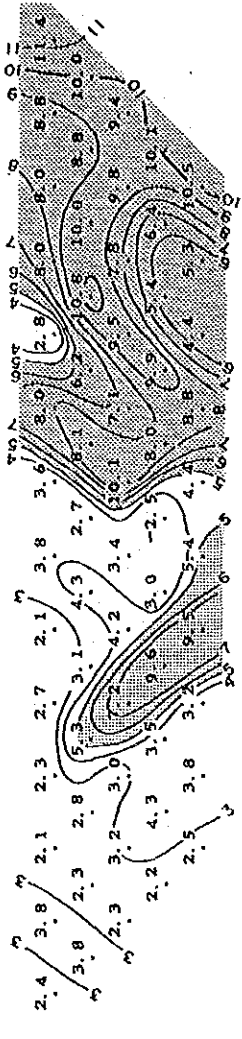
LINE T-1 0 2 4 6 8 10 12 14 16 18 20 22 24 26 28 30 32



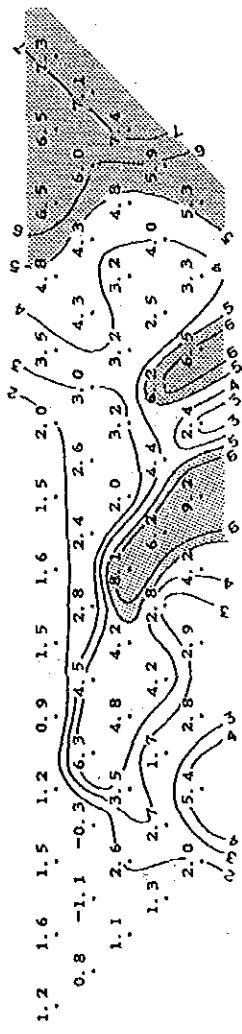
LINE T-2 0 2 4 6 8 10 12 14 16 18 20 22 24 26 28 30 32



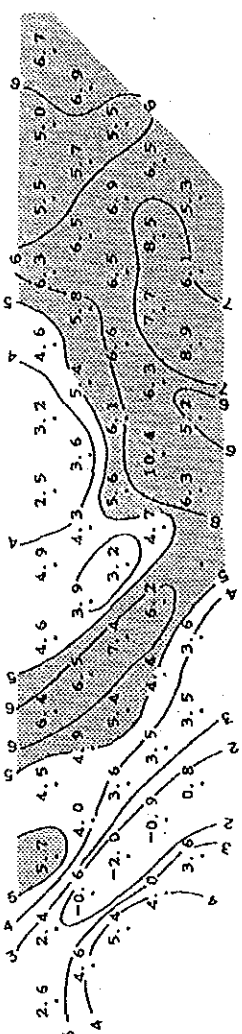
LINE T-3 0 2 4 6 8 10 12 14 16 18 20 22 24 26 28 30 32



LINE T-4 0 2 4 6 8 10 12 14 16 18 20 22 24 26 28 30 32



LINE T-5 0 2 4 6 8 10 12 14 16 18 20 22 24 26 28 30 32



LINE T-6 0 2 4 6 8 10 12 14 16 18 20 22 24 26 28 30 32

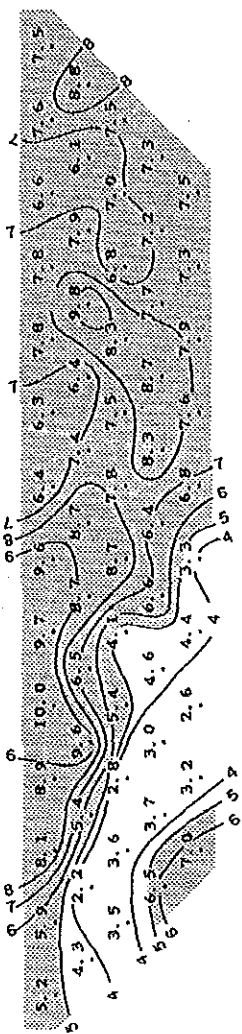


Fig.II-2-12 Pseudo-section of frequency effect of the Telimbela area

In the highly potential area comprised by hornblende-quartz diorite distribution and by its surrounding zone, low FE is seen in n=1 plan map, while high FE anomalies V and VI are seen in n=3 map. Both of them show one side pants-leg shaped anomaly in the middle depth, reflecting a high FE source near stations No.10, 16 and 20 on Line T-3.

Abnormal values are seen at the depth deeper than n=2. One is caused by an electromagnetic coupling (EM coupling) effect or artificial structure (pipeline etc.). The other one is caused by typographical effects which indicates a low S/N ratio due to low potential. Measured points with bigger uncertainty values are as follows:

Line name	n=2	n=3	n=4	n=5
T-1	station No.8	9,11,17	10,12	
T-2		18		
T-3		18	12,16	13
T-4	6,8,10	15	17	
T-5	6	7	8,18	9

In the course of interpretation, these values were estimated appropriately by using their surrounding values. For example on Line T-5 it is seen as a one side pants-legs shaped anomaly of less than 2.0% between stations No.6 and No.9 as well as a high anomaly of 10.4% FE at n=4 of station No.18.

The former anomaly suggests a metamorphical structure near the surface. Therefore if, this anomaly is ignored, a one side pants-leg shaped anomaly of more than 5% FE can be interpreted from stations No.5 to No.7.

The latter anomaly is estimated to represent the pants-legs shaped anomaly of around 6% FE on n=3 of station No.19.

As a result of the above, the high FE anomalies V and VI can be better interpreted by reducing them by 2 to 3%, and therefore, FE plan maps and sections are constructed on these considerations.

On Line T-1, a shallow pants-legs shaped anomaly indicates a high FE anomaly I on station No.17 where montmorillonite is in surface. This anomaly reflect argillization with pyrite dissemination. However, the high FE anomaly detected in the middle depth at station No.23 and extending from high FE anomaly VI on the Line T-3, is probably due to deep buried mineralization in quartz diorite.

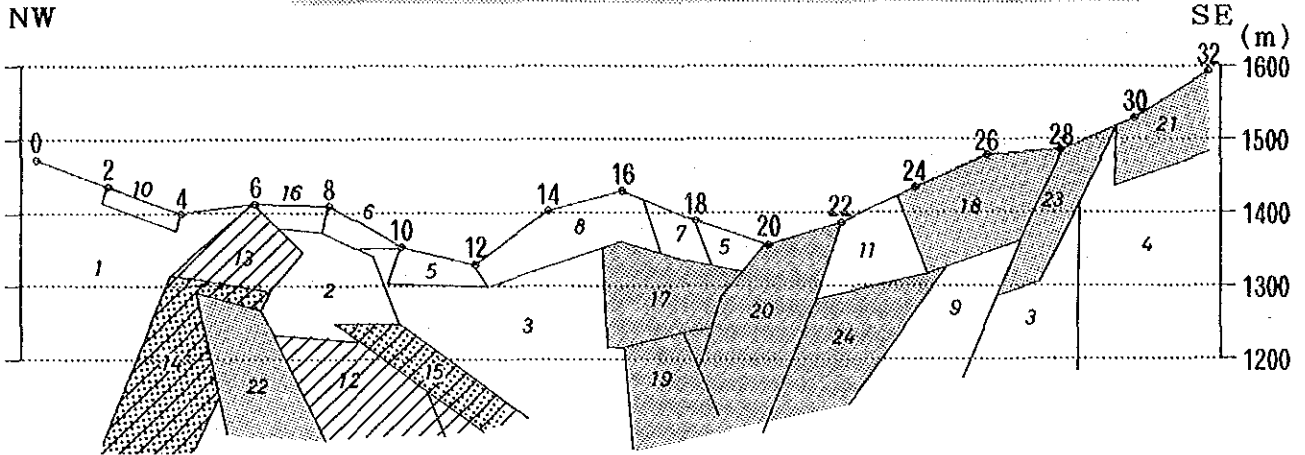
(4) Simulation analysis

The results of model simulation for Line T-3 are shown in Fig.II-2-13.

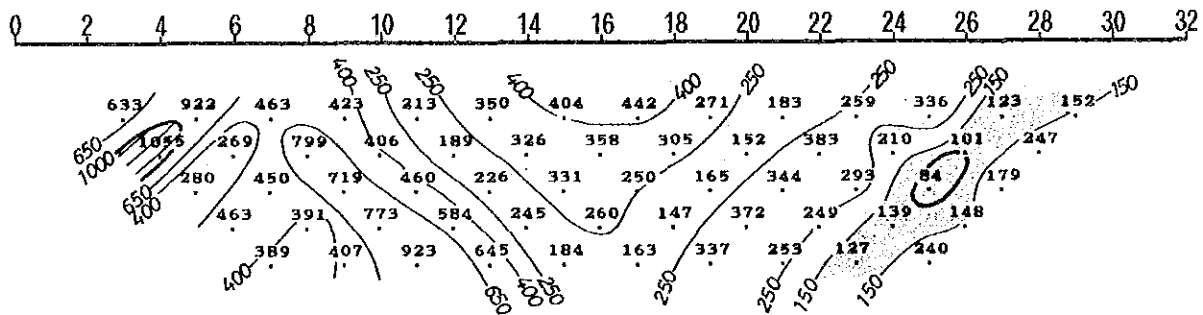
The results of simulation analysis are as follows:

ASSUMED MODEL

CODE NUMBER :	1	2	3	4	5	6	7	8
RESISTIVITY (ohm-m) :	530.0	300.0	200.0	200.0	500.0	100.0	300.0	550.0
P. F. E. (%) :	2.20	1.80	3.50	6.00	1.30	2.00	2.00	2.00
CODE NUMBER :	9	10	11	12	13	14	15	16
RESISTIVITY (ohm-m) :	700.0	450.0	130.0	5000.	2800.	4500.	1500.	550.0
P. F. E. (%) :	2.00	2.50	4.00	1.50	4.00	6.00	15.0	6.50
CODE NUMBER :	17	18	19	20	21	22	23	24
RESISTIVITY (ohm-m) :	400.0	450.0	600.0	300.0	200.0	200.0	70.00	100.0
P. F. E. (%) :	8.00	10.0	15.0	8.50	14.0	15.0	9.00	15.0



APPARENT RESISTIVITY ($\Omega \cdot m$)



PERCENT FREQUENCY EFFECT (%)

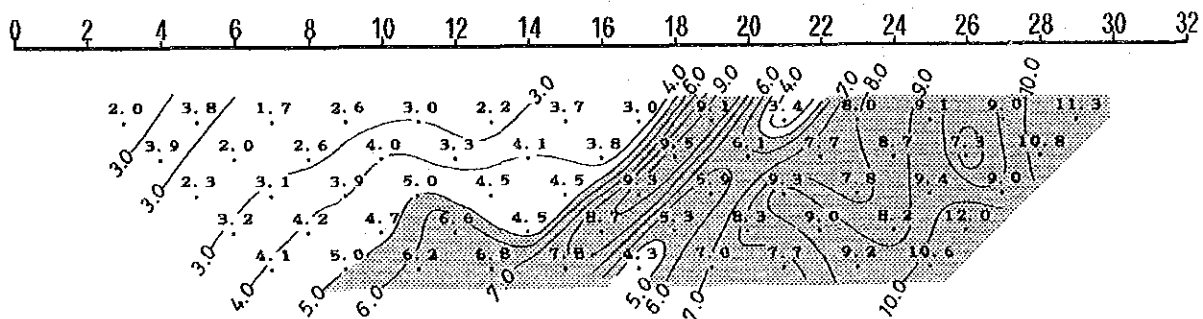


Fig.II-2-13 Analyzed section (line T3) of the Telimbela area

Mostly hidden low resistivity and high FE zone (block codes No.17, 19, 20 and 24) assumed between stations No.16 to No.24, seem to correspond to Ashuaca mineralized zone detected by MJE-9 drill hole. Ashuaca mineralized zone does not seem to be extended from the hole to the northwest, but to the southeast as far as station No.24.

By taking into consideration the geological survey, the low resistivity and high FE zone (No.18, 21 and 23) assumed in the south from station No.24 near the surface, is due probably to strong dissemination of pyrite. On the other hand the hidden resistive body (No.12, 13, 14 and 15) assumed in the stations No.4 to No.10, is suggested to correspond to silicified zone along a fault or hornblende quartz diorite under the Macuchi formation. Low resistivity and high FE zone (No.22) is assumed inside of this body, and high FE zone (No.15) is assumed at the southeastern side.

The mineralization along the creek near the station No.12 is confirmed by the geological survey. However in this simulation analysis, the anomaly source does not suggest to correspond to that mineralization which is probably a small mineralized zone composed of thin veins within the fractures.

Low FE layer (No.5, 6, 7 and 8) assumed at the surface between stations No.8 and 20, with 30-80m in thickness and less than 2.0% of FE, indicates that the reduced FE values are probably due to leached out of mineralization.

2-2-5 Discussion

Apparent resistivity values in this zone range from 38 to 3,370 ohm-m with an average of 349 ohm-m, which are extremely low compared with those detected in Chaso Juan area, and Oshuayco zone of Balzapamba area surveyed by the same method during the Phase II.

Geology of this zone, as in the case of the two above mentioned areas in the Phase II, consists of Macuchi formation with andesite and tuff group, and granitic intrusives. However, in these two areas, silicification which is a cause of high resistivity was the dominant process, while in this year survey, argillization (chloritization and montmorillonitization), which cause low resistivity, seems to be the dominant process. Moreover, in the two areas of the Phase II, because of the dominant silicification is accompanied with mineralization, the mineralized zone reflects high resistivity and high FE. However, in this area, according to physical property tests, the close relation found between mineralization and argillization permitted to understand that the grouping of low resistivity and high FE becomes an important factor for the understanding of mineralization process in this report.

In this section, the simulation analysis carried out on parts of lines T-4, T-5 and T-6 had the purpose of giving an estimate of the high FE anomalies located in area of the unknown mineralizations (western part of survey area). These results are shown in Figs. A-9-1, A-9-2 and A-9-3.

As described in section 2-2-4 (3), the abnormal values caused by EM coupling, artificial structures and or low S/N ratio, are seen at the depth deeper than $n=2$.

These values present difficulties to be simulated by this analysis, however if simulated, the assumed model indicates unrealistic values of FE. In the simulation analysis, it is clearly seen that by reducing 3-4% of FE from the abnormal values of more than 8% indicated below, good realistic model can be obtained.

Line T-3: $n=4$ of station No.12, $n=5$ of station No.13

Line T-4: $n=3$ of station No.15, $n=5$ of station No.17

Line T-5: $n=4$ of station No.18

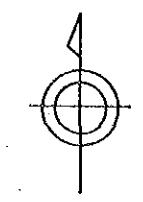
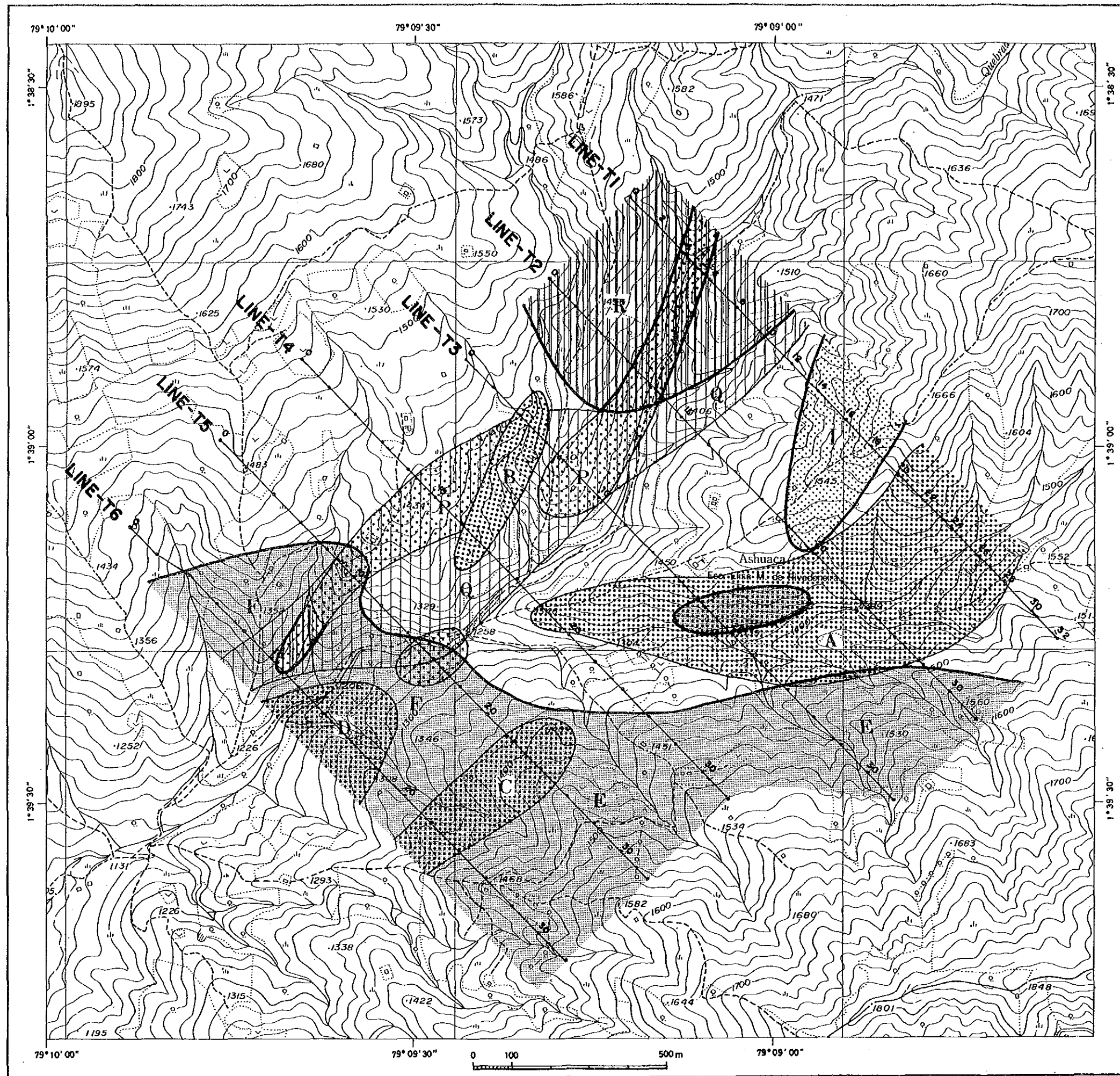
As shown in Fig.A-9-2, a value of less than 1.0% of FE, is considered to be the effect of artificial structure, which if ignored, a pants-legs shaped anomaly can be assumed. This anomaly reflects a low resistivity and high FE layer at the stations No.8 to No.10 on the surface.

Interpreted results by taking into consideration the quantitative analysis, is shown in Fig.II-2-14. Results of present geophysical survey can be summarized according to the results of geological survey, as follows:

1) High FE anomalies V and VI are interpreted as the results of a buried mineralized body in hornblende-quartz diorite distributed in the center of this district and including its surrounded chalcopyrite and pyrite disseminated area. A resembling low resistivity pattern corresponding to chalcopyrite and pyrite disseminated zone are seen along the southern and western creeks of Ashuaca.

2) High FE anomaly VI is interpreted as tongue shaped low resistivity and high FE zone A (100-600 ohm-m and 8.0-20.0% FE), which is from station No.22 on Line T-1 to station No.19 on Line T-4 in the south of Ashuca ridge. This zone crop out on the surface, and deepens westwards and northeastwards.

3) Northern resistive body R is in the zone of quartz diorite. And hidden resistive zone Q is suggested to reflect silicification, detected along a NE-SW fault, from station No.10 on Line T-1 to station No.10 on Line T-6. Inside of these resistive zone, high FE part P



LEGEND




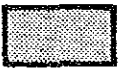


- RESISTIVE ZONE
 -  SURFACE
 -  HIDDEN
 -  HIGH FE (> 6%)
- CONDUCTIVE ZONE
 -  SURFACE (> 5% FE)
 -  HIDDEN (> 10% FE)
 -  MEDIUM RESISTIVITY & HIGH FE

Fig.II-2-14 Interpretation map of the Telimbela area

with more than 5%, is found from station No.5 on Line T-1 to station No.11 on Line T-6. Moreover, hidden low resistivity and high FE zone B (200 ohm-m and 13.0-15.0% FE) is suggested from station No.7 on Line T-3 to station No.13 on Line T-4, crossing the high FE P. These high FE zone corresponded to the high FE anomaly V in the depths.

4) In the surface of Asuaca ridge, low FE layer assumed with 30-80 m in thickness and 2.0% of FE, is indicated leaching out of mineralization in weathered layer. Moreover, confirmed mineralization along Q.Ashuaca is inherited small mineralized zone consisting of thin veins on fracture zone.

5) In the south district, melanocratic quartz diorite is interpreted with 200-250 ohm-m and 4.0-6.0% FE. That mineralization and argillization is suggested as stronger than the other intrusive rocks. And High FE layer is assumed in southeastern end of Lines T-2 to T-6. Moreover, hidden low resistivity and high FE zone (200 ohm-m and 20.0% FE) is assumed at the part of contact with Macuchi formation, between station No.23 on Line T-5 and station No.22 on Line T-6. This zone correspond to high FE anomaly IV, is not conformed mineralization.

6) In the surface of southwestern district (station No.8 to No.10 on Line T-5 and station No.4 to No.20 on Line T-6), low resistivity and high FE layer F corresponded to high FE anomaly III is interpreted with 20-60m in thickness, 80-300 ohm-m and 7.0-12.5% FE. This layer is suggested dissemination with sulfide in Macuchi formation. And under the layer F in station No.12 to No.17 on Line T-6, another low resistivity and high FE zone D assumed with 60 ohm-m and 9,0% FE, extend to depths of southeast and have a possibility to continue southeastwards.

7) High FE anomaly I between station No.12 and No.19 on Line T-1, is typical shallow anomaly with pants-legs shape. This anomaly is considered to reflect montmorillonitization with pyritization near surface, because montmorillonite is detected by geological survey at PT-02 and PT-04 in the northeast of Ashuaca.

2-3 Drilling survey

2-3-1 Purpose of drilling survey

The purpose of the drilling survey is to clarify the mineralizing condition in the deeper part of the mineralized outcrops which were confirmed through detailed geological survey.

2-3-2 Details of drilling survey

(1) Area for drilling work

The "Ashuaca mineralized zone", where drilling survey was conducted, is situated in the central part of northeast zone of Telimbela area, which is nearly 1.5 km northeast of Telimbela village. The drilling sites were located on a steep slope between 1,400 m and 1,500 m above sea level. The sites were selected based on results of Phase III detailed geological survey and geophysical IP method electric survey, comprehensively.

The locations of these holes are shown in Fig.II-2-1.

(2) Outline of drilling work

For this work, principal drilling machine and equipments were donated from Japan, and drilling tools, bits, rods and mud materials including water pumps were brought in from Japan, mud pumps and other supplemental materials from INEMIN. Drilling work was conducted through a period from October 12, to November 11, 1990.

The Model of drilling machine used was the Longyear model L-38. Works for site preparations, equipment dismantling and relocating were proceeded on a daytime shift only. Drilling work was carried out as a rule for 24 hours a day. Wire line process was adopted to improve recovery of drill cores and efficiency of other works. Through the drilling survey required appropriate camp facilities for laborers. Drilling performance of each hole is listed on Table A-6.

(3) Delivery of material and equipments, and preparation of drill sites

Materials and equipments supplied from Japan and INEMIN were delivered to the base in Santa Lucia, which base is constructed as a heliport for Phase III survey. Most of machines and materials such as drilling machine, pumps, mastle, rods and etc. were transported from the base to drilling sites by helicopter, and a few tools and materials were only carried in with manpower. Water required for drilling work was supplied by pumping up from Q. Ugshacocho through high pressure resistive water hose lines.

(4) Drilling work

Actual drilling work is shown in Fig.II-2-15. The progress of drilling work for each hole is shown in Figure A-7, and the drilling equipments and consumed materials are shown in Figure A-8. Detailed works of each hole are as follows:

1) MJE-8

0 to 33.00 m

(hole diameter 101 mm, with NQ-NU casing down to the depth of 33.00 m)

To drill surface soil and gravel layers, 101 mm metal bits and diamond shoe bits were used with bentonite mud water. Surface soil and gravel layers continued until 24.00 m, below this level hornblende quartzdiorite appeared. When reached the country rock at 33.00 m, NQ-NU casing was inserted.

33.00 to 195.50 m

(hole diameter 75.70 mm of NQWL, with BW casing down to 196.00 m)

Through NQWL process, drilling was conducted with use of bentonite mud and TK60B. Lithology was hornblende quartzdiorite with short intervals of andesite of melanocratic quartzdiorite. At the depth of 53.40 m circulating mud water was lost completely, then TK60B was adopted to seal cracks and to recover the un-preferable condition. No return of mud water, however, was achieved. Down to 195.50 m proceeded drilling operation carefully with pumping out mud water through the system, then inserted BW casing.

195.50 to 301.00 m

(hole diameter 60.00 mm of BQWL)

Through BQWL process, drilling was conducted with mud water of TK60B and fresh water. Lithology was hornblende quartzdiorite with andesite xenoliths occasionally. Drilling was completed at the depth of 301.00 m.

2) MJE-9

0 to 28.00 m

(hole diameter 101 mm, with NQ-NU casing down to 28.00 m)

Surface soil and gravel layers were drilled with metal bits and diamond shoe bits, diameter of which was 101 mm. At the depth of 10.00 m circulating mud water was lost completely, "Telstop", a material for sealing cracks, was adopted to recover the un-favorable

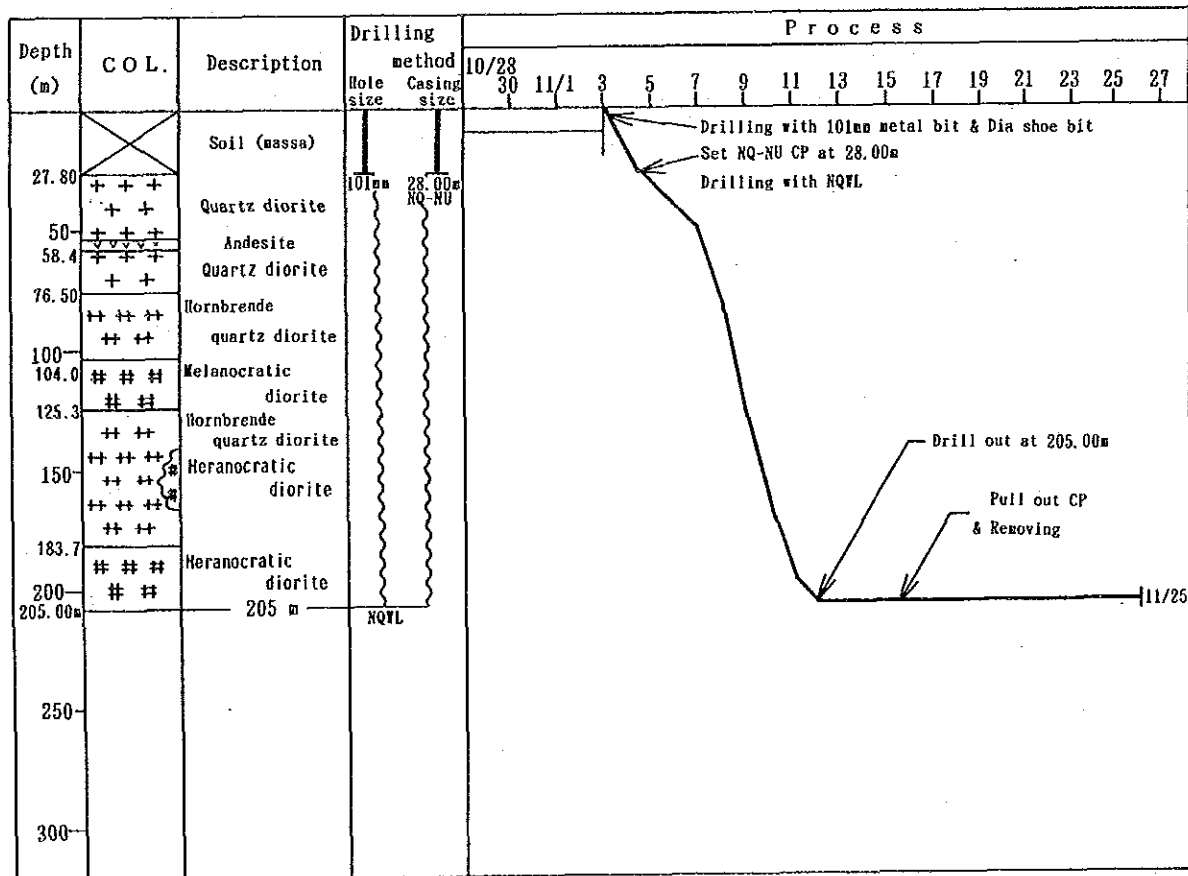
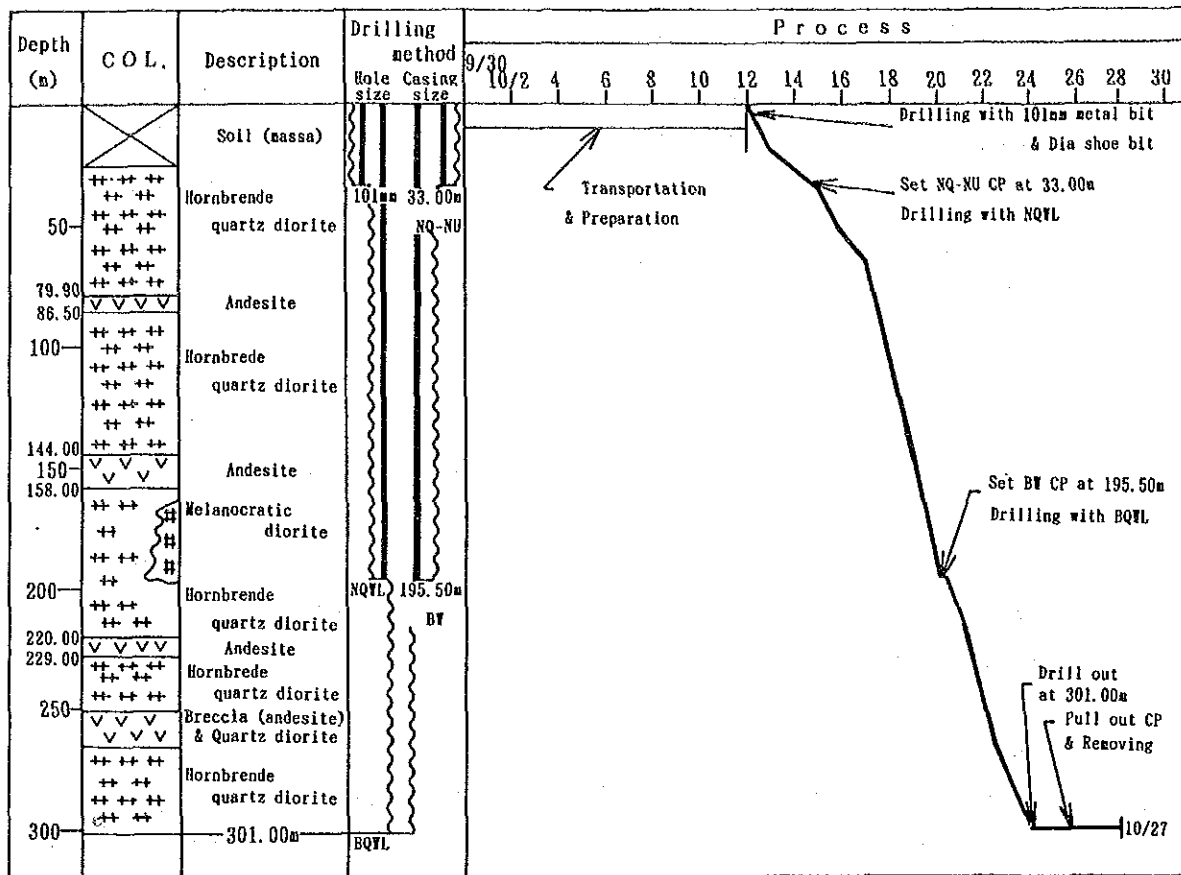


Fig.II-2-15 Progress record of MJE-8 and 9

condition. No return of mud water, however, was achieved. Drilling process was continued carefully with pumping out mud water to the depth of 27.80 m, where drill hole reached the country rock body. Therefore NQ-NU was inserted and fixed at the depth of 28.00 m.

28.00 to 205.00 m

(hole diameter 75.70 mm of NQWL)

Through NQWL process, the hole was drilled with use of fresh water and TK60B. Lithology was hornblende quartzdiorite mainly with andesite, coarse biotite-hornblende quartzdiorite, and melanocratic quartzdiorite occasionally. Immediately below 28.00 m, circulating mud water was lost completely again. Some efforts were made to recover the condition with "Telstop", no return of mud water, however, was achieved. Under such condition, drilling operation was continued down to 205.00 m, at which drilling was completed.

(5) Examination of drill cores

For each hole, drill core examination were proceeded simultaneously with drilling operation at the drilling site and Telimbela base camp. Result of this examination were compiled into columnar section of a scale 1 to 200, which are shown in Plates II-2-2 and II-2-3. Drill cores were split with diamond cutter after completing each drill hole. One half of them was taken for test samples and the other left for duplicate.

2-3-3 Results of drilling survey

In the course of selecting the drilling site, following information were considered comprehensively: the results of detailed geological investigation and IP method electrical survey, both of which were carried out prior to drilling survey.

MJE-8 hole was drilled nearly at the center of the "Ashuaca mineralized zone" which was confirmed to consist of a number of mineralized outcrops accompanying chalcopyrite and pyrite. A principal group of outcrops consists of disseminated and networked zones of mineralization which develop in an area of about 50 m wide and 350 m long, extending in E-W direction.

Mineral paragenesis of the mineralized zone is a assemblage of chalcopyrite-pyrite-(molybdenite)-secondary biotite-chlorite-quartz. And these minerals occur in the interstices of brecciated parts of quartzdiorite as well as in xenoliths of andesite. Breccias of the host rock (HQd) are chloritized and silicified generally.

Surface around MJE-8 and MJE-9 is weathered intensely and covered with thick soil layer. Therefore, no geological and mineralogical information is available whether the rock is mineralized partly or completely.

Pit survey was adopted on the ridge area to acquire any information on the mineralization by observing surfaces of country rocks and/or collecting ore or soil (layer-"C") samples for chemical analysis. Investigation inside of pits revealed that limonite-quartz veinlets be common at the ridge top and rich in copper.

The mineralization, which is confirmed to be intense enough at the river floor of Q. Ugshacocha and Q. Ashuaca, is still desirable level of metal contents at the ridge top where drilling sites are located, the difference of altitude between them, river floor and ridge top for MJE-8 and 9, are 120 m and 150 m respectively.

IP anomaly in the vicinity of drill hole sites (MJE-8 and 9) were as follows: High Frequency Effect of 8 % and High Resistivity of 400 ohm-m. Brief explanation of both drill holes are as follows (see Fig.II-2-16):

(1) MJE-8

Location:

Latitude distance 9817.17 N

Longitude distance 707.40 S

Elevation ASL +1,400 m

Inclination: -90° (vertical)

Depth: 301.00 m

0 to 24.0 m

Masa of hornblende quartzdiorite

24.0 to 79.0 m

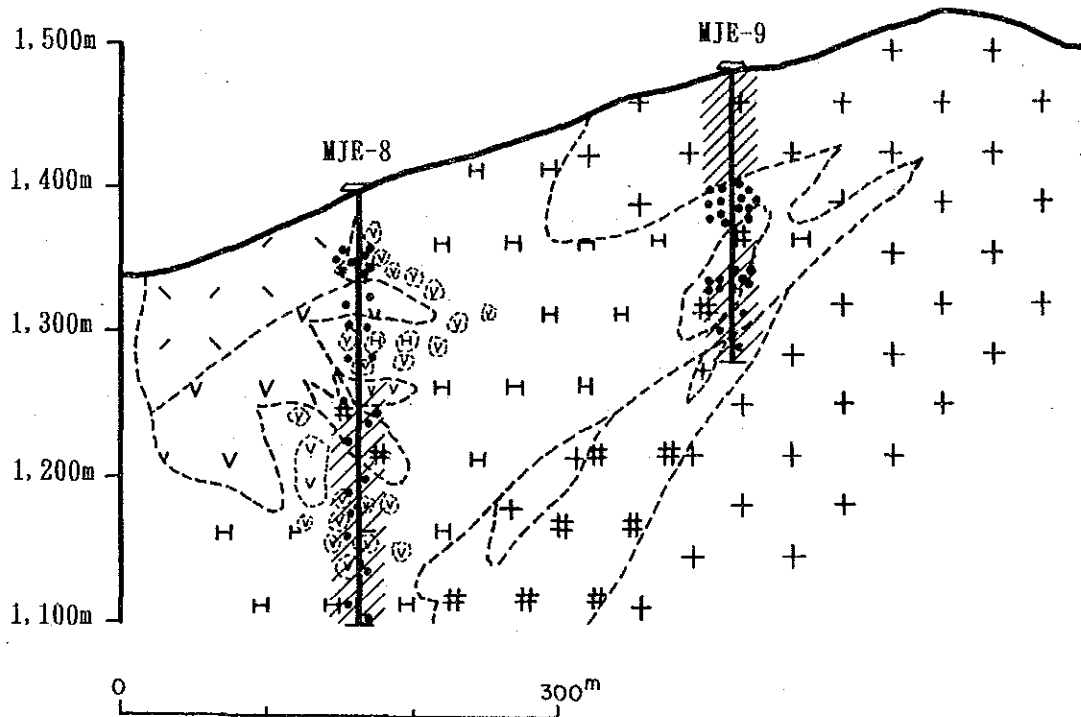
Pale green massive compact hornblende quartzdiorite (HQd). Contains breccias of andesite-hornfels as xenoliths, and brecciated intrusive rock (HQd) itself. Throughout the interval recognized are dissemination, films and/or patches of chalcopyrite and pyrite.

Hornblende-quartzdiorite (HQd) is recognized to be biotized intensely under the microscopic observation at the depth of 55.0 m. Rock forming minerals are also deformed by shear. Plagioclase altered partly to chlorite and epidote.

Polished section revealed that chalcopyrite was precipitated isolated mineral grains as large as 1 to 1.5 mm in diameter filling interstices of rock forming minerals and containing rounded micro grains (0.1 to 0.2 mm in diameter) of pyrite.

79.9 to 86.5 m

Hornfels-andesite. Mineralized in the form of dissemination and films of chalcopyrite



LEGEND

Maevali Formation	B Member	QAn	Quartz bearing andesite	Intrusive Rocks	Qd	Fluorapatite - K-feldspar quartz dikes
		BII	Andesitic pyroclastic rocks		D1	Malakoprosite dikes
		AAm	Andesite		HQd	Basalt - andesite quartz dikes
	A Member	ATI	Andesitic pyroclastic rocks		•••	mineralized zone
		ABT	Basalt andesite flow tuff		≡≡≡	siliceous zone
			///	argillized zone		

Fig.II-2-16 Geologic section of MJE-8 and 9

and pyrite.

86.5 to 144.0 m

Pale green hornblende quartzdiorite (HQd) contains breccias of hornfels-andesite as xenoliths, and brecciated intrusive rock (HQd) itself. Throughout the interval, recognized are dissemination, films (and/or patches) of chalcopyrite and pyrite. The microscopic characteristics are that the host rocks are suffered intensely by propylitization, that deformation of rock forming minerals by shear, that albitization and epidotization of plagioclase, and that complete chloritization and epidotization of biotite.

144.0 to 154.4 m

Dark gray andesite (An). Intense chloritization. Mineralized in the form of dissemination of chalcopyrite and pyrite.

154.4 to 161.6 m

Pale green hornblende quartzdiorite (HQd). Contains breccias of hornfels-andesite. Mineralized slightly in forms of dissemination and films of chalcopyrite and pyrite.

161.6 to 193.3 m

Dark gray to black medium grain, massive compact melanocratic quartzdiorite (DI). Intercalates four sheets of hornblende quartzdiorite, core lengths of which varies from 1.1 to 5.3 m. Mineralized in forms of dissemination (and films partly) of chalcopyrite and pyrite.

193.3 to 220.0 m

Pale green hornblende quartzdiorite (HQd). Contains a number of breccias of hornfels-andesite. Mineralized slightly in forms of dissemination (and films partly) of chalcopyrite and pyrite.

220.0 to 229.2 m

Dark green andesite (An). Intense chloritization with mineralization in the form of films of chalcopyrite and pyrite. Quartz thin veins are also developed.

229.2 to 242.8 m

Pale green hornblende quartzdiorite (HQd). Partly chloritized and argillized. Mineralization in forms of dissemination and films of chalcopyrite and pyrite.

242.8 to 247.4 m

Dark bluish green andesite (An). Mineralized slightly in the form of dissemination of pyrite and chalcopyrite.

247.4 to 251.4 m

Green hornblende quartzdiorite (HQd), intense chloritization. Mineralized in the form of dissemination of chalcopyrite and pyrite.

251.4 to 265.0 m

Dark bluish green andesite (An). Brecciated completely and intruded by hornblende quartzdiorite along fractures. Mineralized slightly in the form of dissemination of pyrite and chalcopyrite.

265.0 to 301.0 m (Bottom)

Greenish blue hornblende quartzdiorite (HQd). Contains locally a number of breccias of andesite. Mineralized in the form of chalcopyrite and pyrite.

(2) MJE-9

Location:

Latitude Distance	9817.26 N
Longitude Distance	705.67 E
Elevation	1,470 m

Inclination: -90°

Depth: 205.00 m

0 to 27.8 m

Masa of biotite-hornblende quartzdiorite.

27.8 to 76.5 m

Gray, coarse, massive compact quartzdiorite (Qd). Contains a number of andesite breccias locally. Mineralized in the form of dissemination of pyrite, and only a few chalcopyrite.

76.5 to 104.0 m

Bluish green, medium grain, hornblende quartzdiorite (HQd). Mineralized in the form of dissemination of pyrite, chalcopyrite and molybdenite. Chloritization and epidotization

are common throughout the interval.

Microscopic observation in thin section of host rock (HQd) at the depth of 100 m revealed that the rock was propylitized intensely, and that rock forming minerals were deformed obviously by shear.

Plagioclase altered slightly to albite and epidote while biotite altered completely to chlorite and epidote.

Polished section of mineralized part at the depth of 93.2 m revealed dissemination of chalcopyrite of 0.1 to 0.3 mm in diameter or finer, and isolated pyrite grains of 0.3 to 0.4 mm in diameter. No magnetite was observed in the section.

104.0 to 125.3 m

Dark bluish green melanocratic quartzdiorite (Di). Intense hornfelsinization (with distinctive secondary biotite).

Mineralized in the form of dissemination of pyrite, chalcopyrite and molybdenite. Chloritization and epidotization are common.

125.3 to 169.4 m

Bluish green hornblende quartzdiorite (HQd). Contains locally breccias of dark bluish green porphyritic (and melanocratic) quartzdiorite. Mineralized in forms of dissemination and films of pyrite, chalcopyrite and an infinitesimal quantities of molybdenite. Chlorite and epidote are also recognized commonly.

169.4 to 205.0 (bottom)

Dark greenish blue melanocratic quartzdiorite (Di). Dark green hornblende quartzdiorite intruded into this interval with a core length of 9.2 m. Mineralized slightly in the form of dissemination of pyrite and chalcopyrite. Chlorite and epidote are also recognized commonly.

2-3-4 Discussion

1) MJE-8

Considerable amount of chalcopyrite and pyrite have been observed on the cores from near surface through bottom of the hole.

Assay result of the interval between 21 m and 102 m in depth revealed as follows:

Core length 81 m, tr to 6.0 g/t of Ag; 0.02 to 0.72 % of Cu, average 0.468 % of Cu.

Adding this, mineralized parts which contain copper contents more than 0.1 % are:

0.29 % of Cu from 108 m to 110 m; 0.12 % of Cu from 124 m to 132 m; 0.32 % of Cu from 170 m to 172 m.

Intensely Cu-mineralized part of the hole are recognized not only where the host rock includes a number of breccias of the Macuchi Formation but also where the host rock is brecciated itself completely.

Cu-mineralization is confirmed to exist down to the bottom of the hole.

2) MJE-9

Through the core of MJE-9, Cu-mineralization of chalcopyrite accompanying with pyrite and molybdenite, are observed as intensely as MJE-8.

Mineralized parts more than 0.1 % Cu are as follows:

Tr to 2.6 g/t of Ag; 0.10 to 0.32 % of Cu, average 0.229 % of Cu from 80 to 105 m; 0.1 to 4.7 g/t of Ag; 0.08 to 0.55 % of Cu, average 0.207 % of Cu from 124 to 161 m.

Adding those mineralized part assay result more than 0.1 % Cu are as follows: 0.19 % of Cu from 36 to 37 m; 0.12 % of Cu from 52 to 53 m; and 0.17 % of Cu from 116 to 117 m.

2-4 Consideration of the survey result in Northeast zone, Telimbela area

1) "Ashuaca mineralized zone" cropped out in and along Q. Ugshacocha river contains chalcopyrite, pyrite and molybdenite. Hornblende quartzdiorite, which intruded into biotite quartzdiorite, has been determined its age and revealed to be 14.5 Ma. Therefore, hornblende quartzdiorite is now considered to be younger than any other intrusive rocks ever observed in this Project area.

2) Intense mineralized part of the zone are exist in and near the fracture structure. And principal ore-minerals are to be chalcopyrite and molybdenite adding to pyrite.

3) Drill hole MJE-8 and 9 revealed that considerable amount of chalcopyrite are still observed at and near the bottom of the holes.

Those minerals were precipitated in the open spaces of cracks of Hornblende quartzdiorite body.

4) IP anomalies are delineated at the northern and southern Ashuaca mineralized zone.

They are considered to be some indication of deeper mineralized zone which extends horizontally and vertically from mineralized outcrops observed along the Q. Ugshacocha and Q. Ashuaca.

Exact position of which are apart slightly from these drill holes MJE-8 and 9.

5) Moderate IP anomaly was pointed out through the course of processing geophysical data, and considered to indicate pyrite dissemination in the melanocratic quartzdiorite body, which distributes widely to the southern part of Ashuaca. This pyrite disseminated zone situates, macroscopically, as a outer part (pyrite rich zone) of the mineralized area.

6) A IP anomalous zone with low conductivity and high FE "called anomaly F" is picked up. Anomalous zone consists of two anomalies, one is of shallow part and the other of deep. Former corresponds to pyrite disseminated zone observed at surface outcrops, but latter may be, possibly, of blind deposits.

7) A IP anomaly distributed to the north of Ashuaca shows shallow part anomaly, which corresponds to extensive montmorillonite zone accompanying with pyrite mineral.

Therefore potentiality of deposit is low.

8) Ashuaca area including drill hole sites (MJE-8 and 9) is expected to have potentiality of mineral ore deposits.

MJE - 8

DRILLING LOG
BALZAPAMBA AREA

Coordinates : 88° 47' N
Elevation : 200 m
Direction : 90°
Inclination : 90°
Total Depth : 300 m

Depth (m)	Core No.	Description	Remarks
0	100
10	101
20	102
30	103
40	104
50	105
60	106
70	107
80	108
90	109
100	110
110	111
120	112
130	113
140	114
150	115
160	116
170	117
180	118
190	119
200	120
210	121
220	122
230	123
240	124
250	125
260	126
270	127
280	128
290	129
300	130

MJE - 8

DRILLING LOG
BALZAPAMBA AREA

Coordinates : 88° 47' N
Elevation : 200 m
Direction : 90°
Inclination : 90°
Total Depth : 300 m

Depth (m)	Core No.	Description	Remarks
0	100
10	101
20	102
30	103
40	104
50	105
60	106
70	107
80	108
90	109
100	110
110	111
120	112
130	113
140	114
150	115
160	116
170	117
180	118
190	119
200	120
210	121
220	122
230	123
240	124
250	125
260	126
270	127
280	128
290	129
300	130

Fig. II-2-17 Drilling Log of MJE-8 in Northeast zone, Balzapamba area

PART III CONCLUSIONS AND
RECOMMENDATIONS

Chapter 1 Conclusion

The third year survey of the Bolivar Project, in the Republic of Ecuador, was conducted for the purpose of delineating mineral deposits by clarifying surrounding geology in the following two areas, the Osohuayco zone of Balzapamba area and the Northeast zone of Telimbela area:

For the Osohuayco, Balzapamba area, detailed geological survey and drilling survey were carried out and for the Northeast, Telimbela area, detailed geological survey, geophysical survey (IP method) and drilling survey were also carried out. The results of the survey are as follows:

1-1 The Osohuayco zone, Balzapamba area

The geology of the area consists of Macuchi Formation and granodiorite which intruded into Macuchi Formation.

Two mineralized zones are recognized in this area, one is Osohuayco North mineralized zone and the other Osohuayco South mineralized zone. Drilling survey was carried out to disclose geological and mineralogical conditions of the IP anomaly which showed high apparent resistivity and high FE (more than 5 %) around the Osohuayco South mineralized zone, as a result of previous year geophysical survey. Any mineralization, however, associating with skarnization was not encountered. Drill hole intersected disseminated mineralized zone of chalcopyrite and pyrite in hornfelsinized andesite of Macuchi Formation (AAn). The assay disclosed the grade of the mineralized zone to be very low at a whole, actual range was 0.01 to 0.18 Cu (average 0.05 % Cu).

1-2 Northeast zone, Telimbela area

The geology of the area consists of Macuchi Formation and Granites which intruded into the Macuchi Formation. Granites are composed of Hornblende-biotite quartzdiorite, hornblend quartzdiorite, melanocratic quartzdiorite dike and coarse quartzdiorite dike. Those rock bodies are distributed and arranged in the NE-SW direction.

Porphyry copper type mineralized zone in the surveyed area is proved to be as a dissemination and network zone of chalcopyrite and pyrite.

These mineralized zones are macroscopically lined up in the direction of NE-SW and mineralization is centered in Hornblende quartzdiorite and affects thoroughly such country rocks as Macuchi Formation intensely.

Mineralized outcrops scatter in the area of 1.5 km X 1.0 km in and along Q. Ugshacochoa

and Q. Ashuaca, high grade ores are notably distributed in an area of 400 m X 600 m close to the Ashuaca school, where dissemination and network zone of chalcopyrite and pyrite are recognized to exist not only in quartzdiorite but also in Macuchi Formation intensely. Moreover, molybdenite is observed in forms of dissemination and/or films scattered.

The assay revealed that southern mineralized part cropping out along Q. Ugshacocha contains 0.71 to 1.38 % Cu and that northern mineralized part cropping out along Q. Ashuaca 0.78 to 0.89 % Cu.

Outer part of the mineralized zone is to be dissemination and network zone of pyrite only. As a result of IP method electric survey, distinguished were 6 of high FE anomalies. FE anomaly corresponds generally to mineralization, while high resistivity anomaly to silicification and low resistivity to argilization.

Drilling survey was conducted at the west and east of the Ashuaca school, results of which are as follows: On the drill hole core MJE-8, intense dissemination of chalcopyrite and pyrite was observed through the hole (from the surface to the bottom).

Principal mineralized zones encountered by drill hole are interval between 21 to 102 m in depth with 0.02 to 0.72 % Cu (average, 0.468 % Cu). Adding this, several other intervals are recognized to show copper contents more than 0.10 %.

Mineralization tends to be dominant in the parts of angular xenoliths of andesite and in the the parts of auto-brecciated zone of quartzdiorite.

On the drill core MJE-9, intense mineralization of chalcopyrite and pyrite was observed through the hole from the surface to the bottom (205.00 m in depth).

Principal mineralized zones encountered by drill hole are intervals between 80 to 105 m in depth with a grade of 0.10 to 0.33 % Cu (average, 0.229 % Cu) and between 124 to 161 m with a grade of 0.08 to 0.55 % Cu (average, 0.207 % Cu). Adding those mineralization, several intervals are also recognized, which show copper contents more than 0.10 %.

As a whole, MJE-9 contains less andesite breccias and shows less auto-brecciation. Therefore, average grade of mineralized parts of MJE-9 was relatively lower than that of MJE-8.

To conclude data and information described above following three mineralized zones are delineated as potential zones of mineralization:

1) "Ashuaca mineralized zone"

As a result of geological survey, a number of intense mineralization of chalcopyrite and pyrite have been recognized around Ashuaca school. IP method electric survey disclosed that the deep low resistivity-high FE anomaly "A" which corresponds to the "Ashuaca

mineralized zone".

Moreover, low apparent-resistivity anomaly was recognized at the intense mineralized parts of chalcopyrite-pyrite in and along Quebradas, west and south of Ashuaca.

2) Ugshacocha mineralized zone

Ugshacocha mineralized zone distributes about 500 m southeast of Ashuaca school. Through detailed geological survey, recognized is intense mineralization of chalcopyrite-pyrite, while this mineralization is confirmed to be corresponded to low resistivity-high FE zone "A" which has been selected as a tongue shape anomalous zone extending from the Northeast of the Ashuaca to the Southeast.

3) Las Tres Cruces mineralized zone

Las Tres Cruces mineralized zone is distributed about 600 m western northwest of Ashuaca school.

As a result of geological survey, intense pyrite dissemination accompanying chalcopyrite are recognized. Furthermore, low resistivity-high FE anomaly "B" is delineated as a narrow and elongated zone with the direction of NNE-SSW by IP method electric survey.

This anomaly implies that hidden mineralized zone may exist in the depth of Macuchi Formation.

Chapter 2 Recommendation for the future survey

Based on the findings of Phase III survey, the following recommendations are made for the future survey.

(1) Osohuayco zone, Balzapamba area (Fig.III-2-1)

The Osohuayco North mineralized zone, mineralized outcrops of which are confirmed through geological survey of Phase III, is extensive in scale and comparatively high grade in copper content.

This mineralized zone occurs in hornblende-biotite granodiorite (Gd). Distribution area of these mineralized outcrops corresponds with the IP anomaly area delineated on the high resistivity-high FE values of Phase II geophysical survey.

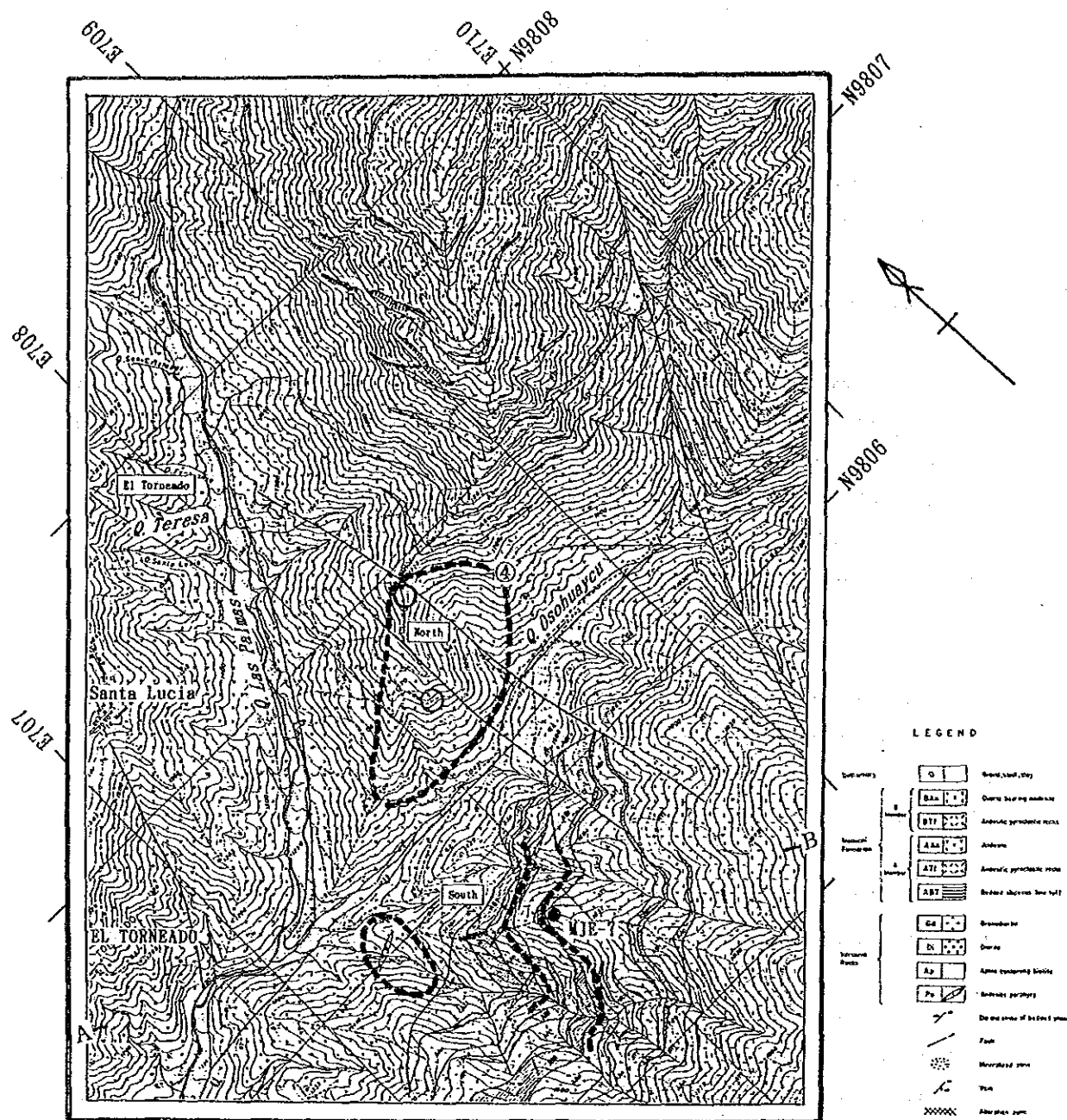
Therefore, drilling survey is recommended to disclose the condition and extent of mineralization in detail, the locations of which are shown in Fig.III-2-1. For example, 300 m deep X 2 holes in Osohuayco North mineralized zone.

(2) Northeast zone, Telimbela area (Fig.III-2-2)

"The Ashuaca mineralized zone", which is confirmed thoroughly by Phase III geological, geophysical and drilling survey, is extensive in scale and high in grade of metal (copper) content. This mineralized zone is also proved to have close relationship of distribution with hornblende quartzdiorite (HQd). Adding this, potential areas have been delineated around "Ashuaca mineralized zone".

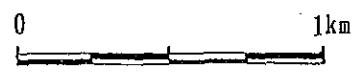
Furthermore, through geophysical survey, IP anomalies are distinguished in the depth of "Ashuaca mineralized zone" where recognized are chain of mineralized outcrops.

Therefore, drilling survey is recommended to disclose the condition and extent of mineralization in detail, the locations of which are shown in Fig.III-2-2. For example, 200 m deep X 3 holes in "ashuaca mineralized zone"; 200 m deep X 2 holes in Ugshacocha mineralized zone; and 200 m deep X 1 hole in Las Tre Cruces mineralized zone.



LEGEND

Tertiary	[Symbol]	Gravel, sand, clay
	[Symbol]	Clayey loess
	[Symbol]	Andean synclinal rocks
	[Symbol]	Andean
	[Symbol]	Andean synclinal zone
Mesozoic	[Symbol]	Andean
	[Symbol]	Andean synclinal zone
	[Symbol]	Andean synclinal zone
Quaternary	[Symbol]	Gravelly
	[Symbol]	Sand
	[Symbol]	Andean synclinal zone
	[Symbol]	Andean synclinal zone
Other symbols		[Symbol] Dashed lines of bedrock
[Symbol]		Fan
[Symbol]		Mineralized zone
[Symbol]		Well
[Symbol]		Algebraic sum



○ Recommended drill point

⊙ Mineralized zone

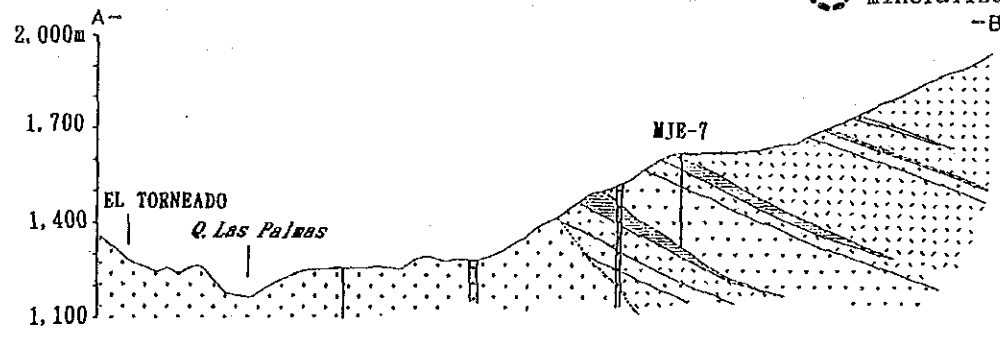


Fig. III-2-1 Recommended area for future survey of the Osohuayco zone, Balzapamba area

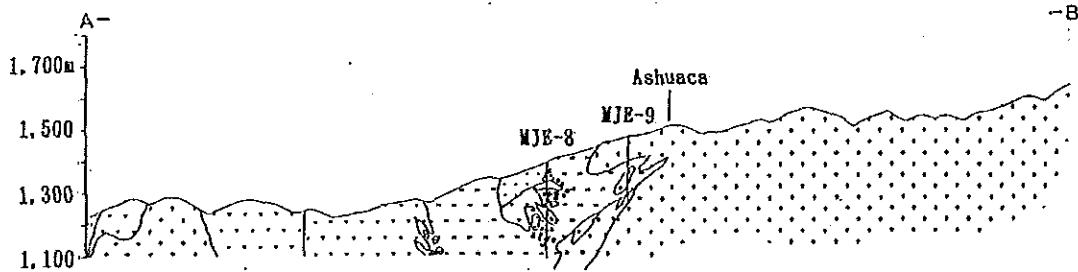
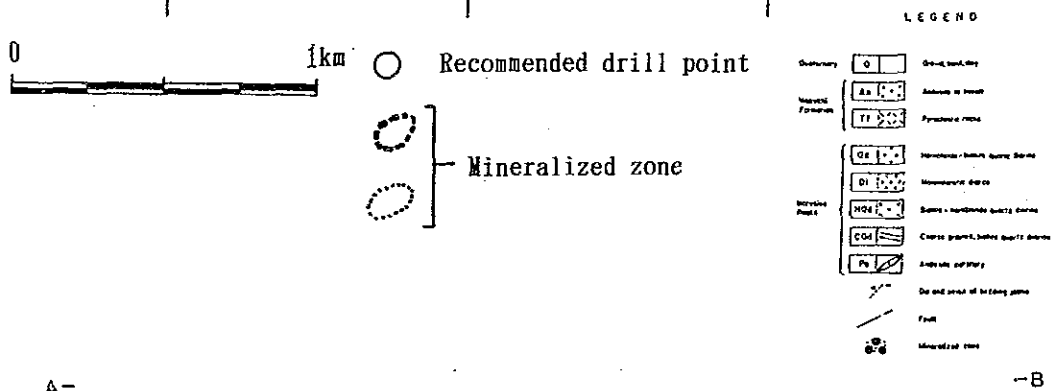
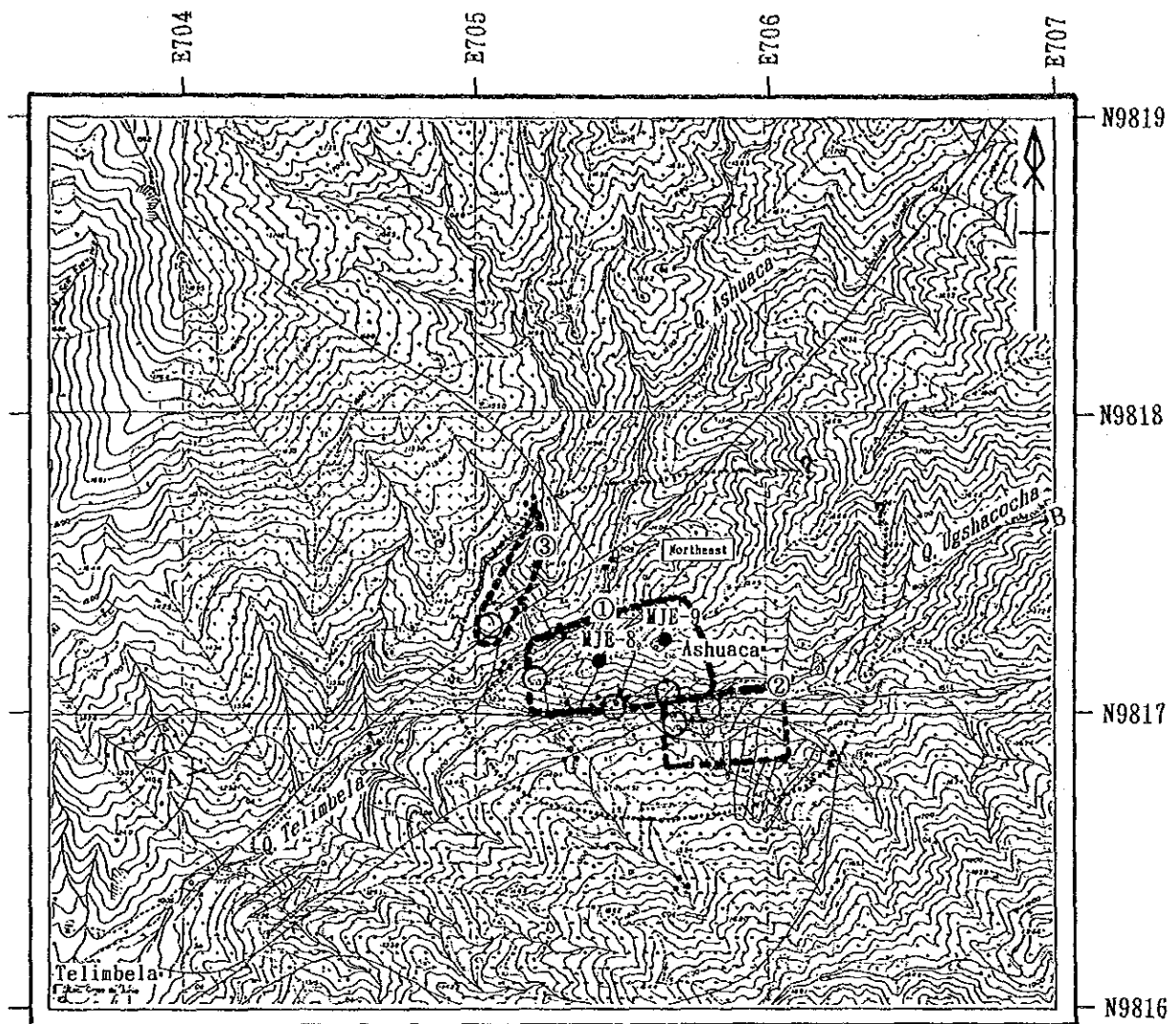


Fig. III-2-2 Recommended area for future survey of the Telimbela area

REFERENCES

1. Bamba, T. y Herrera, J. (1966): Perfil Geologico de los Andes Ecuatorianas, Bull. Geol. Surv. Japan, 17, 18-42 (in Japanese with Spanish and English abstracts)
2. Direccion General de Geologia y Minas/Ministerio de Recursos Naturais y Energeticos (1979): Regional Geochemical Exploration in Western Central Ecuador, 1-19
3. Direccion General de Geologia y Minas/Ministerio de Recursor Naturais y Energeticos (1979): Geochemical, Geophysical and Geological Investigations in Telimbela, Bolivar Province, Western Central Ecuador, 1-34
4. Direccion General de Geologia y Minas/Ministerio de Recursos Naturais y Energeticos (1979): Geochemical, Geophysical and Geological Investigations in San Miguel, Bolivar Province, Western Central Ecuador, 1-18
5. Fairbridge, R. W. (1975): The encyclopedia of World Regional Geology, Part 1: Western Hemisphere, Dowelen, Hutch. Ross., 261-270
6. Farrell, C. W. (1978): Report on the Examination of the La Plata Mine, Ecuador, 1-18
7. Feiniger, T. (1977): Simple Bouguer Gravity Anomaly Map of Ecuador (1:1,000,000)
8. Goossens, P. J. (1969): Mapa Indice Mineralogico del Ecuador (1:1,000,000)
9. Goossens, P. J. (1972): Metallogeny in Ecuadorian Andes, Econ. Geol. 458-468
10. Goldstein, M. A. and Strangway, D. W. (1975): Audio Frequency Magnetotelluric with a Ground Dipole Source. Geophysics vol. 40, p. 669-684.
11. Hall, M. L. and Calle, J. (1982): Geochronological Control for the Main Tectonic-Magmatic Events of Ecuador, Ear. Sci. Rev., 18, 215-239
12. Henderson, W. G. (1979): Cretaceous to Eocene Volcanic are activity in the Andes of northern Ecuador, JI. Geol. Soc. Lond. vol. 136, 367-378
13. INEMIN: Analisis de los Trabajos de Exploracion Realizados en el Centro Occidente del Ecuador (Proyecto Bolivar), 1-28
14. INEMIN (1986): "resumes of 9 projects"
15. INEMIN (1987): Mining in Ecuador
16. Kürzl, M. (1988): Exploratory Data Analysis: Recent Advances for the Interpretation of Geochemical Data, J. Geochem. Explor. 30, 309-322

17. Lepeltier, C. (1964): A simplified Statistical Treatment of Geochemical Data by Graphical Representation, *Econ. Geol.* 64
18. Minera Toachi S. A. (1982): Estudio de Factibilidad, Resumen, Volumen 1-4 La Plata
19. Ministerio de Recursos Naturais y Energeticos/Direccion General de Geologia y Minas (1969): United Nations Development Programme, Survey of Metallic and Non-metallic Minerals, 1-68
20. Ministerio de Recursos Naturais y Energeticos/Direccion General de Geologia y Minas (1979): Mapa Geologico del Ecuador (1:100,000) (49-Guaranda, 50-San Miguel, 51-Bucay)
21. Ministerio de Recursos Naturais y Energeticos/Direccion General de Geologia y Minas (1980): Mapa Metalogenico del Ecuador (1:1,000,000)
22. Ministerio de Recursos Naturais y Energeticos/Direccion General de Geologia y Minas (1982): Mapa Geologico Nacional del Ecuador (1:1,000,000) (Spanish and English)
23. Ministerio de Recursos Naturais y Energeticos/Direccion General de Geologia y Minas (1982): *Geology of Ecuador*, 1-69
24. Ministerio de Recursos Naturais y Energeticos/Direccion General de Geologia y Minas (1982): Informativo Geologico Minero
25. Ministerio de Recursos Naturais y Energeticos/Direccion General de Geologia y Minas (1982): Proyecto Chaso Juan, 1-43
26. Ministerio de Recursos Naturais y Energeticos/Direccion General de Geologia y Minas (1982): Proyecto Balzapamba, 1-23
27. Ministerio de Recursos Naturais y Energeticos/Direccion General de Geologia y Minas: Ecuador Hacia el Desarrollo Minero, 1-91
28. Miyako, T. (1974): Characteristics of Chaucha Porphy Copper Deposit, Ecuador, *Mining Geol.*, 24, 129-135 (in Japanese with English abstract)
29. MME/DNPM (1978): Tectonic Map of South America (1:5,000,000), Explanatory Note 1-21
30. Overseas Technical Cooperation Agency (1963): Report on the Investigation of Ore Deposit at the Macuchi Mining District in Cotopaxi Province of Ecuador, 1-31 (Pl.12, Fig. 15)

31. Puig, C. A. (1984): Ecuador-not only oil, but also mining, *Mining Magazine*, 588-591
32. Sauer, W. (1970): *Geologische Karte von Ecuador (1:1,500,000)*
33. Servicio Nacional de Geología y Minería/Ministerio de Industrias y Comercio (1969): *Mapa Geológico del Ecuador (1:1,000,000)*
34. Sinclair, A. J. (1974): Selection of Threshold Values in Geochemical Data Using Probability Graphs, *J. Geochem. Explor.* 3, 129-149
35. Stewart, J. W., Evernden, J. F. and Snelling, N. J. (1974): Age Determination from Andean Peru: A Reconnaissance Survey, *Geol. Soc. America Bul.* 85, 1107-1116
36. White, W. H., Bookstrom, A. A., Kamilli, R. J., Ganster, M. W., Smith, R. P., Ranta, D. E. and Steininger, R. C. (1981): Character and Origin of Climax-Type Molybdenum Deposits, *Econ. Geol.* 75th Anniversary Volume, 270-316

LIST OF FIGURES

- Fig. I Location map of the project area
- Fig. I-1-1 Location map of the surveyed area
- Fig. I-3-1 Stratigraphic correlation around the project area
- Fig. I-3-2 Geotectonic and metallogenic zone map of Ecuador
- Fig. I-4-1 Generalized stratigraphy of the project area
- Fig. II-1-1 Geological map of the Osohuayco, Balzapamba area
- Fig. II-1-2 Generalized stratigraphic section of the Osohuayco, Balzapamba area
- Fig. II-1-3 Geologic column of Mt Bunque Loma of the Osohuayco, Balzapamba area
- Fig. II-1-4 Geologic column of Q. Osohuayco of the Osohuayco, Balzapamba area
- Fig. II-1-5 Geologic column of the Southern Osohuayco zone, Balzapamba area
- Fig. II-1-6 Mineralization and magnetic susceptibility on a outcrop along Q. Terresa
- Fig. II-1-7 Progress record of MJE-7 of the Osohuayco, Balzapamba area
- Fig. II-1-8 Geologic section of MJE-7 of the Osohuayco, Balzapamba area
- Fig. II-2-1 Geological map of the Telimbela area
- Fig. II-2-2 Generalized stratigraphic section of the Telimbela area
- Fig. II-2-3 Geologic column of northeastern part of Telimbela
- Fig. II-2-4 Geologic sketch of a mineralized outcrop in ZONE V
- Fig. II-2-5 Location map of IP survey lines of the Telimbela area
- Fig. II-2-6 Flow chart of IP data analysis
- Fig. II-2-7 Apparent resistivity plan map(n=1) of the Telimbela area
- Fig. II-2-8 Apparent resistivity plan map(n=3) of the Telimbela area
- Fig. II-2-9 Pseudo-sections of apparent resistivity
- Fig. II-2-10 FE plan map(n=1) of the Telimbela area
- Fig. II-2-11 FE plan map(n=3) of the Telimbela area
- Fig. II-2-12 Pseudo-sections of frequency effect of the Telimbela area
- Fig. II-2-13 Analyzed section (line T3) of the Telimbela area
- Fig. II-2-14 Interpretation map of the Telimbela area
- Fig. II-2-15 Progress record of MJE-8 and 9
- Fig. II-2-16 Geologic section of MJE-8 and 9
- Fig. II-2-17 Drilling log of MJE-8 in Northeast zone, Balzapamba area
- Fig. III-2-1 Recommended area for future survey of the Osohuayco zone, Balzapamba area
- Fig. III-2-2 Recommended area for future survey of the Telimbela area

LIST OF TABLES

Table I -1-1	List of survey amounts
Table I -1-2	List of lavolatory works
Table I -1-3	Member list of project administration
Table I -1-4	Member list of survey team
Table I -2-1	Temperature and precipitation of the project area
Table I -3-1	Classification of metallogenic zones
Table I -4-1	Summary of survey results with mineral showings
Table II -2-1	Resistivity and FE of rock samples in the Telimbela area

LIST OF APPENDICES

Photo A-1	Microphotograph of thin section
Photo A-2	Microphotograph of polished section
FigureA-1	Location map of the samples tested
FigureA-2	Distribution map of the measured magnetic susceptibility
FigureA-3	Location map of the pits tested
FigureA-4	Sketches of Pit-walls
FigureA-5	Interpretation map of lineaments on aerial photograph
FigureA-6	Apparent resistivity plan map (n=5) of the Telimbela area
FigureA-7	Frequency effect plan map (n=5) of the Telimbela area
FigureA-8	Psedo-sections of lines T-1 ~T-6 of the Telimbela area
FigureA-9	Analyzed sections of lines T4 ~T6 of the Telimbela area
Table A-1	Microscopic observations(thin section)
Table A-2	Microscopic observations(polished section)
Table A-3	Assay results of ore samples(geological survey and drill core)
Table A-4	Results of X-ray diffractive analysis
Table A-5	Lists of measured value of IP survey
Table A-6	Generalized drilling results
Table A-7	Summary record of drilling results (MJE-7, 8 and 9)
Table A-8	Drilling equipments and consumed materials

LIST OF PLATES

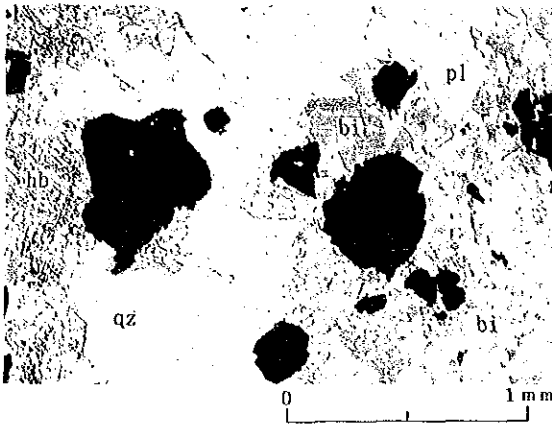
Plate II -1-1	Geological map and profile of the Osohuayco, Balzapamba area
Plate II -1-2	Drilling log MJE-7 (1:200) (1)~(2)
Plate II -2-1	Geological map and profile of the Telimbela area(1:10,000)
Plate II -2-2	Drilling log MJE-8 (1:200) (1)~(2)
Plate II -2-3	Drilling log MJE-9 (1:200) (1)

A P P E N D I X E S

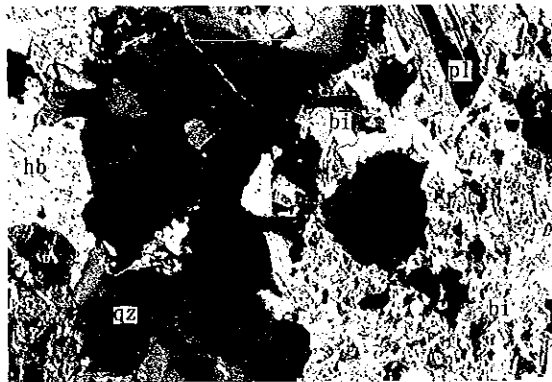
Photo A-1 Microphotograph of thin section

Abbreviation

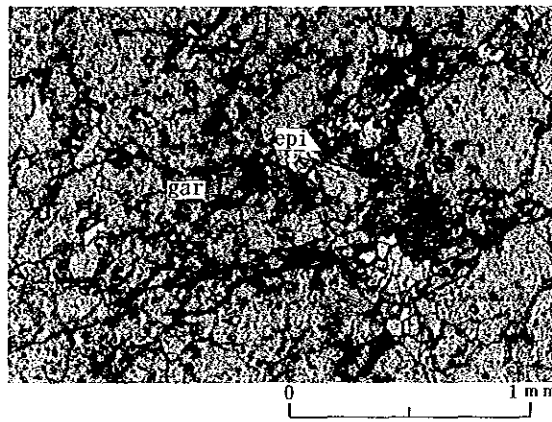
qz	:	quartz
pl	:	plagioclase
kf	:	potash feldspar
mus	:	muscovite
bi	:	biotite
bi(p)	:	biotite(deformed)
bi(h)	:	biotite(biotitization)
hb	:	hornbrende
act	:	actinolite
chl	:	chlorite
epi	:	epidote
cal	:	calcite
gar	:	garnet



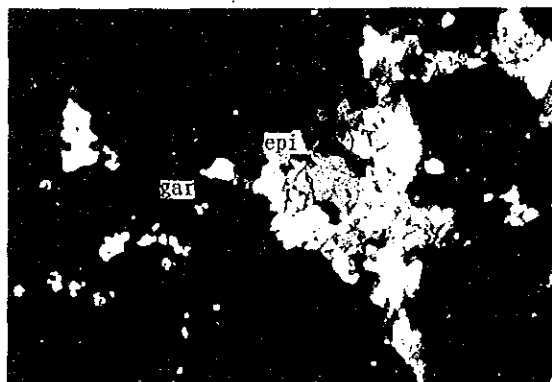
Sample No. : B3043
 Rock name : Hornbrede - (biotite)
 quartz diorite
 Location : Osohuayco
 Texture : Holocrystalline
 altered by biotite
 (only lower polar)



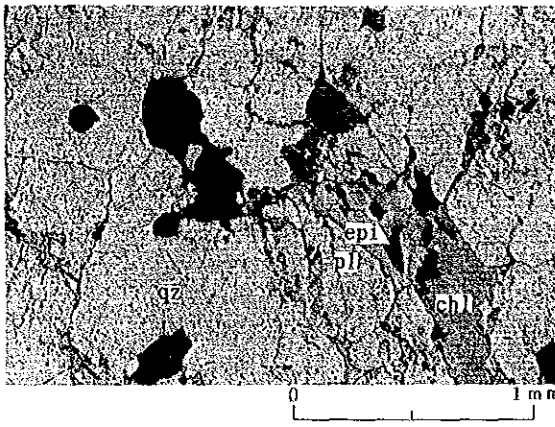
(crossed polars)



Sample No. : C3098
 Rock name : Altered dacitic
 lapilli tuff(?)
 Location : Osohuayco
 Texture : with lithic fragments(?)
 (only lower polar)



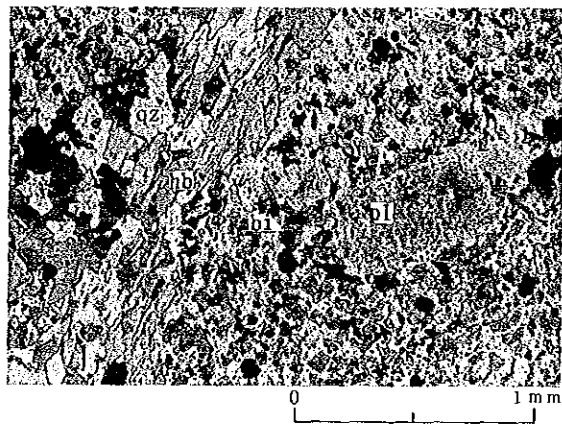
(crossed polars)



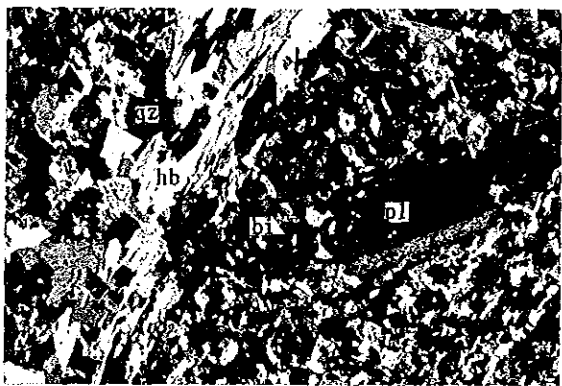
Sample No. : C3001
 Rock name : Garnet skarn
 Location : Osohuayco
 Texture : Massive, granular
 (only lower polar)



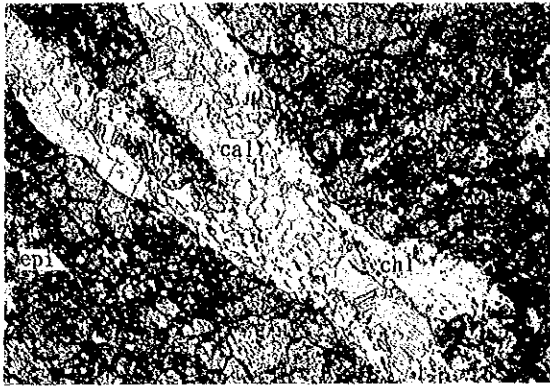
(crossed polars)



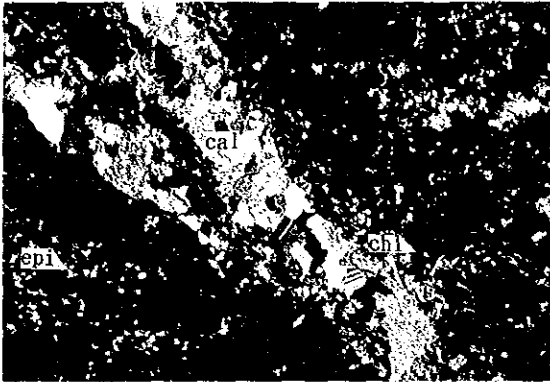
Sample No. : MJE-7 (267.3m)
 Rock name : Contact-metamorphosed
 Hornbrende andesite
 Location : Osohuayco
 Texture : Porphyritic
 (only lower polar)



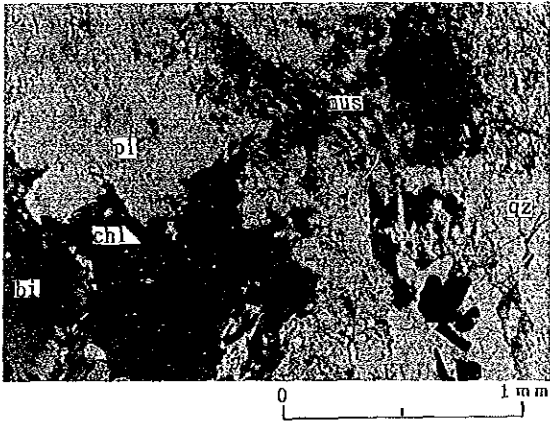
(crossed polars)



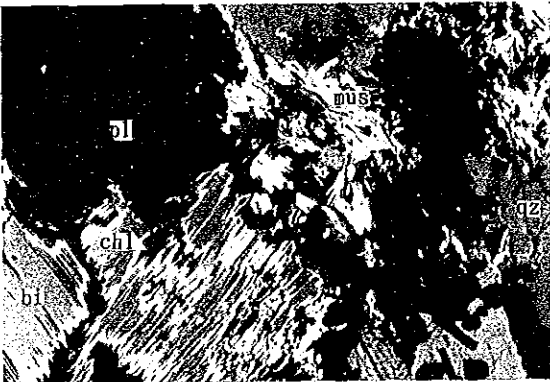
Sample No. : MJE - 7 (98.0m)
 Rock name : Garnet skarn
 with calcite veinlets
 Location : Osohuayco
 Texture : Granular aggregate
 (only lower polar)



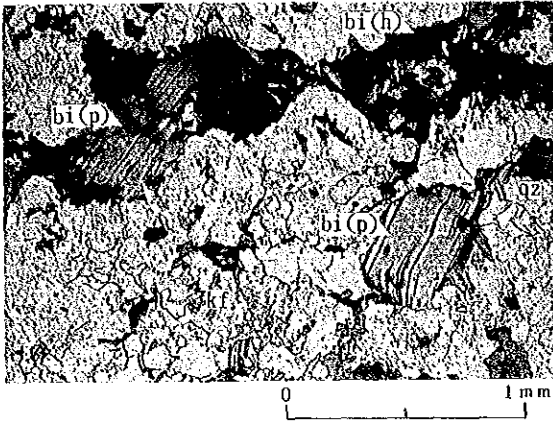
(crossed polars)



Sample No. : C3033
 Rock name : Biotite - hornblende
 quartz diorite
 Location : Telimbela
 Texture : Holocrystalline with
 preferred orientation
 (only lower polar)

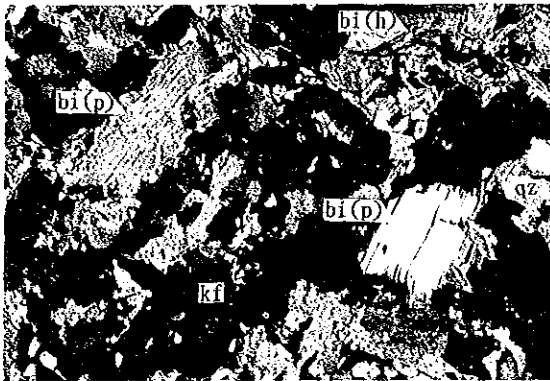


(crossed polars)

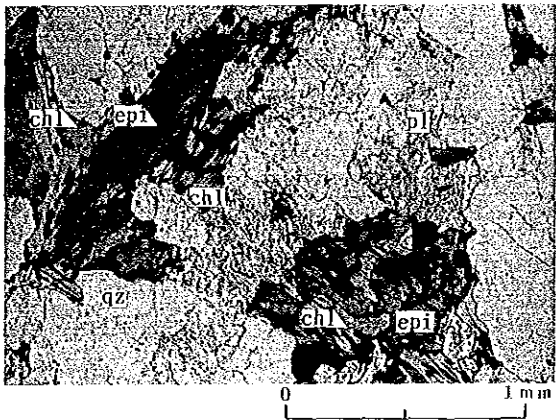


Sample No. : MJE - 8 (55.0m)
 Rock name : Biotite granodiorite
 Location : Telimbela
 Texture : Holocrystalline
 sheared

(only lower polar)

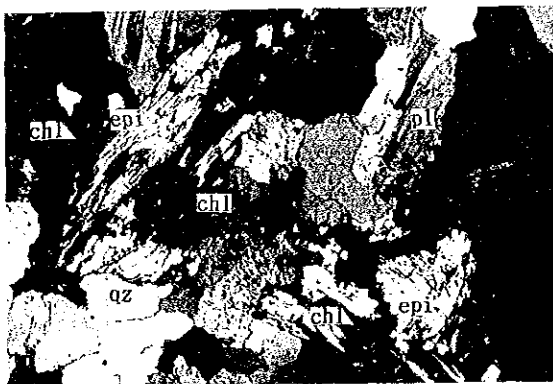


(crossed polars)

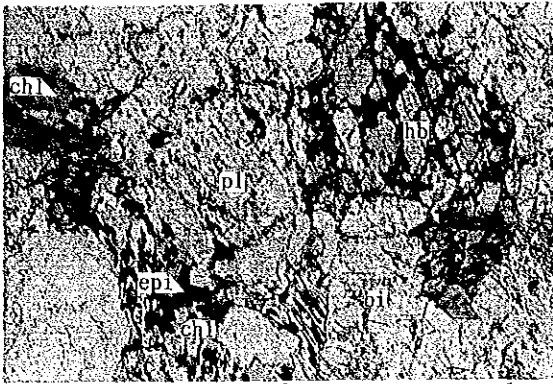


Sample No. : MJE - 8 (119.0m)
 Rock name : Biotite granodiorite
 Location : Telimbela
 Texture : Holocrystalline
 sheared

(only lower polar)

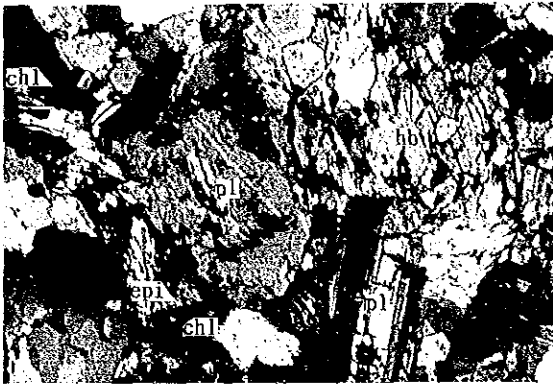


(crossed polars)

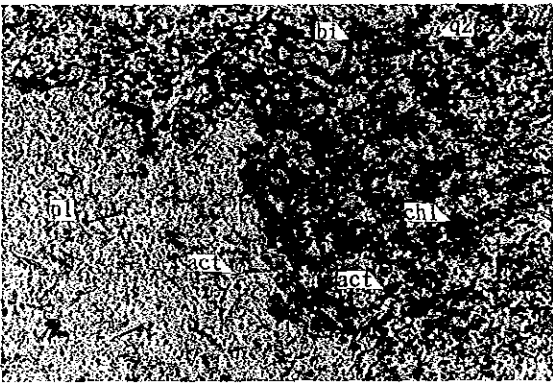


Sample No. : MJE -9 (100.0m)
 Rock name : Hornblende - biotite
 quartz diorite
 Location : Telimbela
 Texture : Holocrystalline
 sheared

(only lower polar)



(crossed polars)



Sample No. : C3050
 Rock name : Biotite quartz diorite
 Location : Telimbela
 Texture : Holocrystalline

(only lower polar)

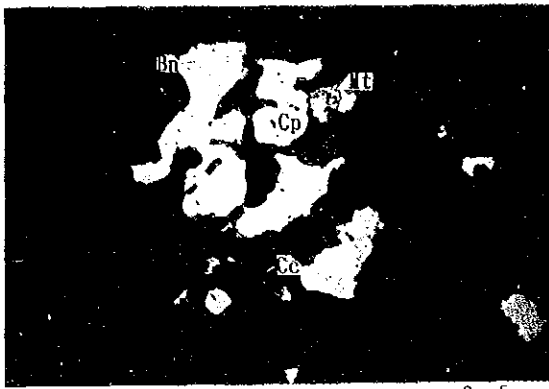


(crossed polars)

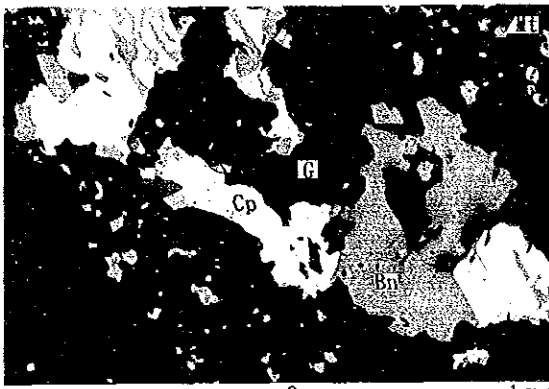
Photo A-2 Microphotograph of polished section

Abbreviation

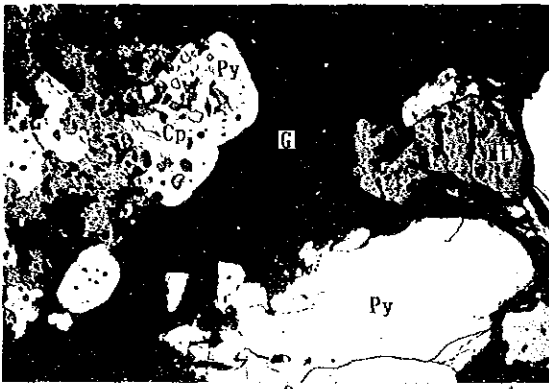
Cp	:	Chalcopyrite
Py	:	Pyrite
Mo	:	Molybdenite
Mt	:	Magnetite
Hm	:	Hematite
Bn	:	Bonite
Cc	:	Chalcocite
Lm	:	Limonite
G	:	Gangue minerals



Sample No. : B3043
 Occurrence : Cp - Mo - Mt dissemination
 Location : Osohuayco



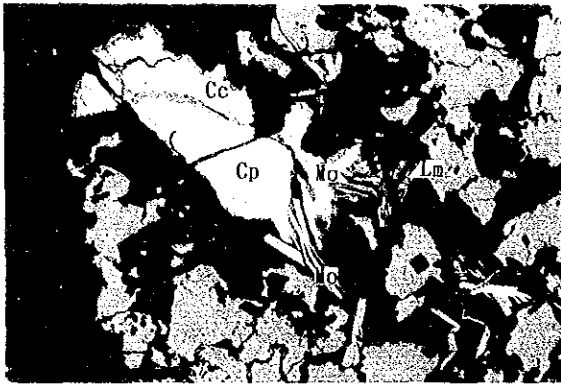
Sample No. : MJE - 7 (245.5m)
 Occurrence : Cp - Py veinlets (~3m wide),
 and Py - Mt dissemination
 Location : Osohuayco



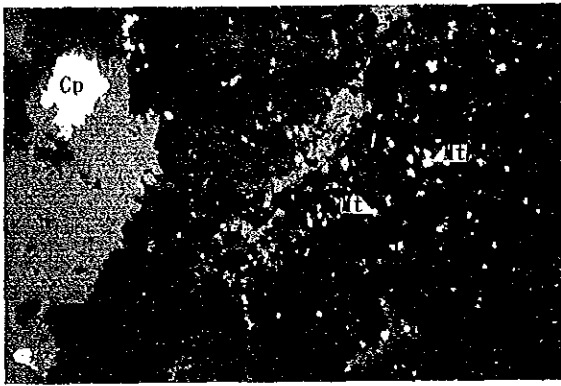
Sample No. : MJE - 7 (267.4m)
 Occurrence : Py - Mt veinlets (~3m wide),
 and Mt dissemination
 Location : Osohayco



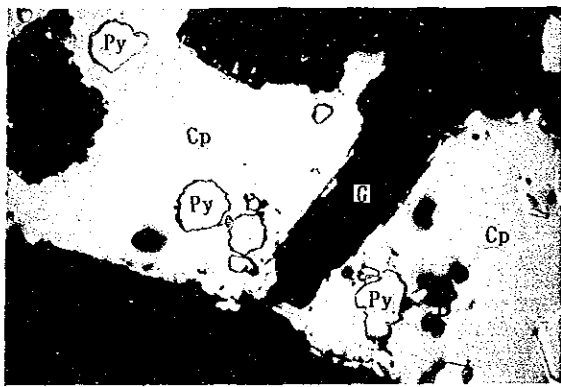
Sample No. : A3027
 Occurrence : Mo - Py - Cp - Mt dissemination
 Location : Telimbela



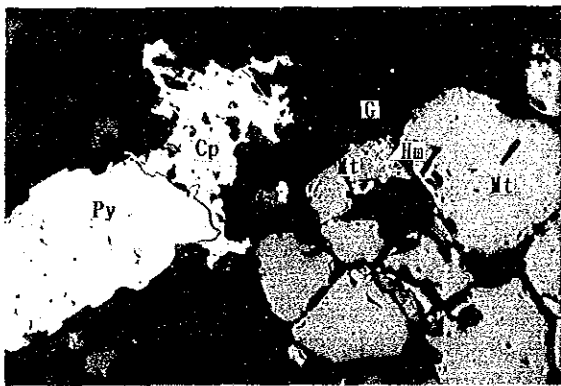
Sample No. : B3005
 Occurrence : Cp - Py veinlets (1mm wide),
 and Mt dissemination
 Location : Telimbela



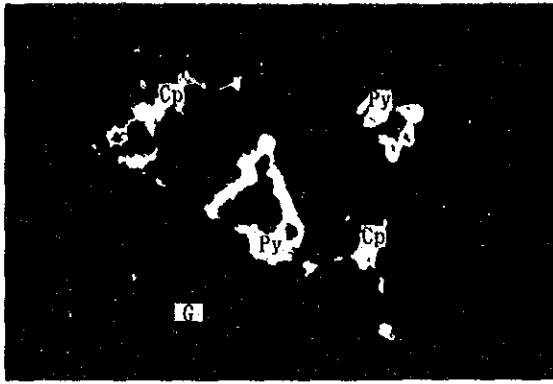
Sample No. : B3018
 Occurrence : Mo - Cp - Mt dissemination
 Location : Telimbela



Sample No. : MJE - 8 (53.8m)
 Occurrence : Cp veinlets
 Location : Telimbela



Sample No. : MJE - 8 (251.1m)
 Occurrence : Py veinlets (~ 2mm wide),
 and Cp, Py, & Mt dissemination
 Location : Telimbela



Sample No. : MJE - 9 (93.2m)
Occurrence : Cp & Py dissemination
Location : Telimbela

Fig.A-1

Location map of the sample tested

